

AMERICAN UNIVERSITY OF BEIRUT

OPTIMAL POWER FLOW WITH STORAGE INTEGRATION

by
JOE AKL TAREK KORBANE

A thesis
submitted in partial fulfillment of the requirements
for the degree of Master of Engineering
to the Department of Electrical and Computer Engineering
of the Faculty of Engineering and Architecture
at the American University of Beirut

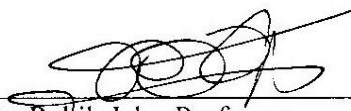
Beirut, Lebanon
September 2014

AMERICAN UNIVERSITY OF BEIRUT

OPTIMAL POWER FLOW WITH STORAGE INTEGRATION

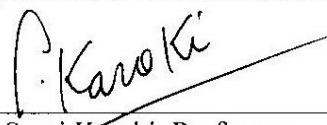
by
JOE AKL TAREK KORBANE

Approved by:




Dr. Rabih Jabr, Professor
Department of Electrical and Computer Engineering

Advisor



Dr. Sami Karaki, Professor
Department of Electrical and Computer Engineering

Member of Committee



Dr. Riad Chedid, Professor
Department of Electrical and Computer Engineering

Member of Committee

Date of thesis defense: September 16, 2014

ACKNOWLEDGMENTS

I would like to express my sincere gratitude to those persons who assisted in making this work a worthwhile experience.

My profound thanks go in the first place to Professor Rabih Jabr, my thesis advisor, who, through his guidance, valuable advice and criticism followed me step-by-step throughout the progress of my work. Professor Jabr supported me with his vast knowledge and academic expertise. This thesis would not have been completed successfully without his efforts and patience.

I would sincerely like to thank also Professor Sami Karaki and Professor Riad Chedid for their valuable encouragement and assistance throughout my work on the thesis.

In addition, I would like to thank my parents and friends for their moral and non-ending support for without them, I would never have achieved what I did.

Finally, I cannot but thank God, who was with me throughout my work, and was watching me day by day.

AN ABSTRACT OF THE THESIS OF

Joe Akl Tarek Korbane for Master of Engineering
Major: Electrical and Computer Engineering

Title: Optimal Power Flow With Storage Integration

This research considers the optimal power flow (OPF) problem in a power system with storage integration. The classical problem formulation requires minimizing the cost of conventional generation by taking into consideration the different time periods over which the renewable generation output varies in addition to the physical and technical constraints of the network. However, the uncertainty associated with the renewable power production forecast is substantial; it can be modeled by an interval set. Affinely adjustable robust optimization is therefore proposed to account for uncertainties in the OPF formulation. The base-point generation is calculated to serve the load when the renewable power production is at its forecasted value, and the participation factors control the generators to ensure a feasible solution for all instances of renewable power output in the predefined uncertainty set. The affinely adjustable robust problem is formulated as a convex quadratic program and tested on standard IEEE networks having 14 and 118 nodes that consider uncertainties over a 24-hour study horizon.

CONTENTS

ACKNOWLEDGMENTS.....	v
ABSTRACT.....	vi
LIST OF ILLUSTRATIONS.....	ix
LIST OF TABLES.....	x
LIST OF SYMBOLS.....	xi

Chapter

I. INTRODUCTION.....	1
A. Motivation.....	1
B. Overview.....	3
II. LITERATURE REVIEW.....	4
III. ROBUST OPTIMIZATION OVERVIEW.....	9
IV. BASIC PROBLEM FORMULATION.....	12
A. Problem Formulation Without RES Uncertainty.....	12
B. Demonstration Example.....	15

V.	APPLYING ROBUST OPTIMIZATION TO THE OPF PROBLEM.....	18
A.	Overview.....	18
B.	Problem Formulation With RES Uncertainty.....	18
C.	Affinely Adjustable Robust OPF.....	20
D.	Demonstration Example.....	22
VI.	SIMULATION RESULTS.....	24
A.	Wind Power Prediction Models.....	24
B.	Numerical Results.....	27
1.	Results for the IEEE 14-Bus Network.....	28
a.	“Advanced” Forecasting Approach.....	28
i.	Fixed Participation Factors.....	28
ii.	Variable Participation Factors.....	30
b.	Persistence Forecasting Model.....	31
i.	Fixed Participation Factors.....	31
ii.	Variable Participation Factors.....	32
2.	Results for the IEEE 118-Bus Network.....	34
VII.	CONCLUSION.....	39
Appendix		
I.	IEEE 14-BUS SYSTEM DATA.....	40
II.	IEEE 118-BUS SYSTEM DATA.....	43
	BIBLIOGRAPHY.....	54

ILLUSTRATIONS

Figure	Page
4-1: 4-bus system.....	16
6-1: Variation of the <i>NMAE</i> in the “Advanced” approach for the three cases.....	26
6-2: Variation of the <i>NMAE</i> in the Persistence model for the five cases.....	27
6-3: Total input and output power of the system for part a.i.....	29
6-4: Total storage energy variation of the system for part a.i.....	29
6-5: Total input and output power of the system for part a.ii.....	30
6-6: Total storage energy variation of the system for part a.ii.....	31
6-7: Total input and output power of the system for part b.i.....	31
6-8: Total storage energy variation of the system for part b.i.....	32
6-9: Total input and output power of the system for part b.ii.....	33
6-10: Total storage energy variation of the system for part b.ii.....	33
6-11: Total input and output power of the 118-bus system.....	35
6-12: Total storage energy variation of the 118-bus system.....	35

TABLES

Table	Page
6.1: CPLEX solution time (seconds) for all the cases studied.....	36
6.2: Total base generation cost (dollars) for all the cases studied.....	36
6.3: Percentage increase in cost relative to the cost without uncertainty.....	38

SYMBOLS

Z	Nonempty convex and compact set.
ζ^t	Vector of uncertain wind output power at a given time period t .
T	Total number of periods studied.
c_{i2}^t	Quadratic cost coefficient of generator i at a given time period t .
c_{i1}^t	Linear cost coefficient of generator i at a given time period t .
G_i^t	Generation for generator i at a given time period t .
$G_{i(base)}$	Base generation for generator i .
ng	Total number of generation units.
nb	Number of buses.
nl	Number of lines.
ns	Total number of storage units.
nw	Number of nodes where wind turbines are connected.
nd	Number of nodes where loads are connected.
B	Nodal admittance matrix of the bus system, with column 1 eliminated.
θ^t	Vector of the bus nodes phase angles for buses 2 to nb at a given time period t .
G^t	$ng \times 1$ vector of generation at a given time period t .
S^t	$ns \times 1$ vector of power flow from the storage units at a given time period t .
P_w^t	$nw \times 1$ vector of generation from wind turbines at a given time period t .
P_d^t	$nd \times 1$ vector of the loads at a given time period t .

B_L	Line admittance matrix of the bus system, with column 1 eliminated.
F^t	Vector of the line power flows at a given time period t .
E_i^t	Energy stored in unit i at a given time period t .
Δt	Length of every time period.
(R_{down}, R_{up})	Generator ramp rates limits.
L	$nl \times (nb - 1)$ matrix of power transfer distribution factors.
W	Matrix of ones.
I	Identity matrix.
I_1	Matrix that maps the vector G^t into the bus connection indexes of an $(nb - 1) \times 1$ vector.
I_2	Matrix that maps the vector S^t into the bus connection indexes of an $(nb - 1) \times 1$ vector.
I_3	Matrix that maps the vector P_w^t into the bus connection indexes of an $(nb - 1) \times 1$ vector.
I_4	Matrix that maps the vector P_d^t into the bus connection indexes of an $(nb - 1) \times 1$ vector.
β_i	Participation factor of generation unit i .
u^t	Vector of non-adjustable variables, representing G_{base}^t and S^t .
v^t	Vector of adjustable variables, representing the algebraic sum of the uncertain power injection variations.
m	Number of rows in the data matrices/vectors U, V^t, A, b^t of the AAROPF formulation.
$\theta_i^T / \bar{\theta}_i^T$	i th row vector in an $m \times nw$ matrix of positive/negative slack variables.

$\mathbf{\cdot}^T$	Transpose operator.
$diag\{\mathbf{\cdot}\}$	Diagonal matrix with elements in vector $\mathbf{\cdot}$.
$\mathbf{\cdot}^{min/max}$	Minimum/maximum magnitude operator.
$\mathbf{\cdot}_i$	Element i in vector $\mathbf{\cdot}$ or row i in matrix $\mathbf{\cdot}$.
$\mathbf{\cdot}_{ij}$	From bus node i to bus node j .
k	Prediction time-step.
$\hat{P}_p(t + k t)$	Future wind predicted production made at time origin t .
$P(t)$	Last measured wind power value.
$e(t + k t)$	Prediction error.
$P_{wi}^t(actual)$	Actual wind output power from wind generator i for time period t .
P_{wi}^t	Wind power output forecast from wind generator i for time period t .
ζ_i^t	Wind power forecast error from wind generator i for time period t .
N	Number of data points used for the model evaluation.
P	Average measured wind power production.
x	Real parameter used in the equation of the power forecast error curve.

CHAPTER I

INTRODUCTION

A. Motivation

Due to the increase in power demand, the conventional sources needed to generate electricity are going to deplete in the near future. In addition, the cost of power production from conventional sources is increasing; however, the cost of renewable energy is decreasing. As a result, it is important to restructure the electric power industry and integrate renewable energy sources such as wind and solar energy. However, this process is challenging because the renewable sources require some mitigation strategies to maintain consistent electric power delivered through the network. Therefore, distributed energy storage is needed and has to be studied as an important strategy. There are many advantages behind using this technique including but not limited to decreasing the need for installing new transmission lines and generation units, providing energy reserves and indirectly protecting the environment due to integrating renewable energy sources in the power grid. The role of energy storage in power systems has been widely researched, investigated and tested through simulations since 1981 when a design project used the hybrid simulator in order to study the effects of battery storage in a power system. Battery and inverter models were developed for that simulator and were added to a power system simulation with generation units [1]. Later on, mitigating the effects of renewable energy sources by using energy storage elements has been of great concern to researchers despite the fact

that energy constraints exist. Taking into consideration the deployment of renewable energy sources, energy storage is becoming important in power systems [2].

Moreover, the idea of micro-grids has been developed where distributed renewable energy sources, loads and energy storage are integrated in a reliable and economic way [3]. In [4], different feasible electricity storage technologies are compared for their importance over different time scales. Moreover, [5] proposes a methodology for allocating an energy storage system (ESS) in a power distribution system containing wind energy penetration and discusses how to efficiently allocate the storage for minimizing the curtailed wind energy. In order to store the surplus of power coming from renewable sources and use it during the low power generation time or when the cost of generation is relatively high, energy devices have to be installed at different locations in the power system. In fact, the appropriate storage technology to be used together with the required capacity and the charge/discharge rates are the subject of recent research [6].

This thesis presents an adjustable robust optimization approach to account for the uncertainty of renewable energy sources (RESs) in the presence of storage units in the optimal power flow (OPF) problem over a 24-hour study horizon. It proposes an affinely adjustable robust OPF (AAROPF) formulation, where the base-point generation is calculated to serve the load, and the generation control, through participation factors, guarantees a feasible and optimal solution for all the realizations of RES output within a defined set of uncertainty. The AAROPF problem is solved using quadratic programming and manages the computations of the base-point generation as well as the participation factors.

B. Overview

Chapter 2 of the thesis provides a general literature review related to the contributions of this research. It presents various optimization techniques to solve the OPF problem that includes RESs and storage units.

In Chapter 3, an overview of robust optimization is presented to deal with problems considering uncertainty. The methodology is explained, and a mathematical model of the problem is given by taking into consideration a prescribed uncertainty set.

In Chapter 4, the OPF problem is formulated without taking into consideration the RESs uncertainty, specifically the output power from wind turbines. A demonstration example of a 4-bus network is then dealt with in which the objective function and the constraints are written.

In Chapter 5, an affinely adjustable robust optimization is applied to the OPF problem by taking into account the uncertainty of the wind output power that can now vary in a definite interval. Then, an example is presented in which the objective function and the constraints are written in the presence of uncertainty.

Chapter 6 reports the results of the simulations obtained by applying two mathematical models that are used for wind power prediction. The simulations are performed by fixing and varying the participation factors of the generators and increasing the range of the uncertainty set. The results are presented and analyzed for the IEEE 14-bus and the IEEE 118-bus networks.

Chapter 7 concludes the thesis by summarizing the main contributions and drawing the most important conclusions out of the simulation results.

CHAPTER II

LITERATURE REVIEW

Extensive research on solving the OPF problem with renewable energy generation and storage integration was reported in the literature. Various optimization approaches to solve this problem have been published.

The OPF problem optimizes a cost function (generation cost as an example) while satisfying the physical and technical constraints of the network. The OPF problem is extended in [6] to integrate charge/discharge rates for the distributed energy storage over the network. Unlike the conventional OPF problem, where the optimization is static and can be solved independent of time, adding storage charge/discharge dynamics makes the optimization dependent of time and coupled between periods, yielding an optimal control problem. Charging occurs when the generation cost is low and discharging occurs when it is relatively high. As for the problem setup, both the active and reactive powers and the node voltage magnitudes at the generation buses are bounded between minimum and maximum values. At every bus, the amount of stored energy and the rate of energy charge/discharge are modeled by a first order difference equation relating both variables with respect to time. In addition, the amount of storage is bounded between zero and a maximum storage value, and the charging/discharging rate is bounded between a minimum and a maximum value. Also, the reactive storage power inflow/outflow at every bus and at any time is bounded between a minimum and a maximum value. So, the OPF problem is subject to the above-mentioned constraints containing the following decision

variables: bus voltages, real and reactive powers, amount of storage, charging/discharging rate and the reactive storage power inflow/outflow with respect to time.

As for the parameters concerned with optimization, they represent the power demand at each bus in a certain time, the upper and lower bounds on the power generation at a certain generation bus, the upper and lower bounds on the bus voltage magnitude, the bus storage capacity, the initial bus storage, the upper and lower bounds on the charging/discharging rates and the bus admittance matrix [10]. This OPF problem with an AC network model is non-convex and is therefore hard to solve.

In [7], a sufficient condition is provided for the problem to be equivalent to a convex problem. Instead of directly solving the OPF problem, its Lagrangian dual problem is solved, which is proved to be a convex semi-definite program (SDP).

Reference [6] extends the SDP to allow including storage dynamics and the computational procedure is used to study the effects of energy storage on generation costs by performing case studies using the IEEE test networks. The formulated equations show that adding the charging/discharging dynamics to the original OPF problem does not change the dual variable structure with no storage dynamics as given in [7]. However, certain constraints such as the thermal line limits are omitted from the problem formulation.

The convex optimization problems present in [6] can be solved using the parser YALMIP and the SeDuMi solver in MATLAB [8], [9].

The purpose behind the work in [6] is to assess the utility of the storage in mitigating many issues related to renewable energy resources integration in the power system.

The OPF problem with energy storage and time-varying generation costs and demands in [11] is modeled as in previous references ignoring reactive power, and thus simplifying the problem formulation. The simplest case of a single-generator-single-load (SGSL) with a battery connected is solved in this reference in order to clearly understand the effect of storage on the optimal generation and battery charge/discharge. In addition, the case of a network with multiple generators and loads is solved.

As far as [12] is concerned, the research work looks at risk mitigated OPF by analyzing a power system including wind power and energy storage penetration. The problem is formulated similar to previous works discussed. However, the OPF's aim is to schedule the use of reserves and the energy storage units with minimum possible operating cost. In addition, the OPF problem can be analyzed to determine the optimal placement of storage through the power network. The authors reached a very important conclusion, which is when there is enough transmission capacity in the power system, it is advisable to use an even distribution of storage that can maximize the power rate delivered by the storage units. On the other hand, it is advisable to store the energy where it is generated when the transmission capacity is limited. In this case, the energy stored is then discharged to feed the load.

A storage device model in [13] is represented by its rated energy, power and efficiency. In the OPF context, power flows from one time to another in the same location, which is the path provided by the storage devices. These devices are considered efficient if they are charged at a low locational marginal price (LMP) and discharged at a relatively high LMP. By examining the economic side, [13] shows that it is possible to minimize the yearly cost of such power system with storage using

stochastic programming, that accounts for the sum of operational and construction costs in a certain year. The study in [13] emphasizes on the cost of adding storage devices to the system, and represents it as a linear construction cost which is a function of rated energy and power. Proper modeling of storage devices improves the efficiency of the system. Therefore, they can be used in studies considering a high penetration of renewable energy resources.

In the framework of power flow planning under RESs uncertainty, optimization can be classified as probabilistic, stochastic, or robust [18]. Probabilistic approaches supplement the calculation of the deterministic OPF control variables with the solution's statistical characteristics computation [19]. Stochastic approaches compute the decision variables by taking into account parameter uncertainty. The early approaches make use of Powell's penalty function method to convert the stochastic OPF to a set of non-linear equations [20]. Recent techniques include combining probabilistic load flow and genetic algorithm [21], Monte Carlo simulation and deterministic optimization [22], and a hybrid genetic algorithm along with a neural network approximating the chance constraints [23]. In [24], closed form solutions are presented for economic load dispatch with stochastic wind; however, the results lack generation limit constraints. There has been recent research that proposes the use of chance constraints to define policies ensuring the wind power generation utilization [25]. The stochastic approaches require the knowledge of the probability density function (PDF) of the uncertain parameters, which is usually not Gaussian, and therefore, hard to acquire [26]. As an example, the wind turbine power curve is non-linear resulting in the fact that the PDF of the wind power prediction is not Gaussian.

Optimal power flow with storage remains the work of present and future research due to its importance in the electrical engineering field and mainly the power sector. By the use of energy storage devices, the power system is more flexible in terms of quality of power, stability and reliability. Moreover, energy storage systems will definitely play an important role in sustained energy in the near future, and plants utilizing renewable resources will develop the economic use of generation along with power transmission.

CHAPTER III

ROBUST OPTIMIZATION OVERVIEW

Robust optimization is a type of optimization that is emerging as a leading methodology to address problems under uncertainty [16]. It should be noted that unknown parameters of the system belong to a non-empty convex, compact and unknown uncertainty set. Reference [14] contains case studies, where robust optimization is applied. The methodology for single-stage robust optimization is to find the robust counterpart (RC) of the OPF problem. Two types of counterparts are commonly used, which are the Interval and the Ellipsoidal robust counterparts. In general, the RC of an uncertain linear optimization problem is not a linear optimization problem because of infinitely many linear constraints. However, there are some cases when the RC is written equivalently to a linear program. This is called the interval model of uncertainty.

It is naturally assumed that different uncertain data are affected by perturbations, which are random and independent of each other. Therefore, the RC based on the interval model of uncertainty becomes too conservative to use because it immunizes the solution against a highly unlikely situation. A less conservative approach is offered by the ellipsoidal model of uncertainty, which is equivalent to a quadratic program.

Reference [17] suggests a two-stage Adjustable Robust Counterpart (ARC) approach instead of applying the single-stage RC approach because the latter often results in very conservative approximations of the uncertain problems addressed. This

reference explains how to form the ARC of a quadratic optimization problem, which is the case of the OPF problem having a quadratic cost function that is studied in this thesis. Part of the variables is not adjustable and is grouped in vector u ; the remaining part can adjust to the uncertain data and is grouped in vector v . An uncertain linear optimization problem can be written under the form:

$$LP_Z = \{ \min_{u,v} \{ c^T u : Uu + Vv \leq b \} \}_{\zeta=[U,V,b] \in Z} \quad (3.1)$$

In (3.1), Z is a nonempty convex and compact set; the uncertain parameter ζ is made up of the matrices U and V and the right hand side b . The ARC of this problem is given by:

$$(ARC) \min_u \{ c^T u : \forall (\zeta = [U, V, b]) \in Z, \exists v \text{ such that } Uu + Vv \leq b \} \quad (3.2)$$

The introduction of the Affinely Adjustable Robust Counterparts (AARC) is motivated for tractable approximations of the ARC for a wide range of the sets under uncertainty. For fixed u , the adjustable variables v of the LP_Z are considered affine functions of the data and represented by:

$$v = w + W\zeta, \text{ where } \zeta = [U, V, b] \quad (3.3)$$

The AARC of the uncertain linear programming problem (3.1) is then defined as the following optimization problem:

$$(AARC) \min_{u,w,W} \{ c^T u : Uu + V(w + W\zeta) \leq b, \forall (\zeta = [U, V, b]) \in Z \} \quad (3.4)$$

The OPF problem under uncertainty is generally defined by:

$$P_\zeta \begin{cases} \min c^T u \\ Uu + Vv \leq A\zeta + b \end{cases} \quad (3.5)$$

In (3.5), U and V are fixed, and the uncertain parameter is represented by ζ .

When the uncertainty set for ζ is defined as a box $\chi = \{\zeta, \text{ such that } \zeta_{min} \leq \zeta \leq \zeta_{max}\}$, then the AARC of the uncertain problem in (3.5) is expressed by the following linear programming problem [17]:

$$LP \begin{cases} \min_{u,w,W,z_i,\bar{z}_i} c^T u \\ U^i u + V^i w - b^i + \zeta_{max}^T z_i + \zeta_{min}^T \bar{z}_i \leq 0, \\ z_i \geq 0, \quad z_i^T \geq V^i W - A^i, \\ \bar{z}_i \leq 0, \quad \bar{z}_i^T \leq V^i W - A^i \end{cases} \quad (3.6)$$

Reference [18] takes into consideration the RESs uncertainty in the OPF problem formulation. It presents an adjustable robust optimization approach and proposes an affinely adjustable robust OPF (AAROPF) formulation. This method aims to calculate the base-point generation that serves the forecast load, which is not balanced by RESs. The participation factors of the generators employed in automatic generation control (AGC) systems guarantee a feasible solution for all the RES output realizations that fall within a specific set of uncertainty. Quadratic programming is used to solve this problem by successive constraint enforcement. An affinely adjustable solution is obtained after the problem minimizes the expected operational cost and produces adjustable variables that are considered affine functions of the RES uncertainty.

CHAPTER IV

BASIC PROBLEM FORMULATION

In the first part of this chapter, the OPF problem is formulated without taking into consideration the uncertainty of the output power from wind turbines. In the second part, an example is included in which the objective function and the constraints are written explicitly.

A. Problem Formulation Without RES Uncertainty

The optimal power flow (OPF) problem in [6] is formulated by applying the DC load flow. So, the reactive storage power inflow/outflow at a given bus node and the line conductance are neglected. Reference [6] does not take into account renewable generation. However, this can be integrated in the model of the problem as a “negative” load.

The setup of the problem is shown below:

$$\text{minimize } \sum_{t=1}^T \sum_{i=1}^{ng} c_{i2}^t (G_i^t)^2 + c_{i1}^t G_i^t \quad (4.1)$$

- c_{i2}^t is the quadratic cost coefficient of generator i at a given time period t .
- c_{i1}^t is the linear cost coefficient of generator i at a given time period t .
- G_i^t is the generation for generator i at a given time period t .
- T is the total number of periods studied.
- ng is the total number of generation units.

The constraints of the formulated problem are the following (4.2)-(4.9):

$$B\theta^t - I_1 G^t - I_2 S^t = I_3 P_w^t - I_4 P_d^t, \quad t = 1, \dots, T \quad (4.2)$$

- B is the nodal admittance matrix of the bus system, with column 1 corresponding to the slack bus eliminated.
- θ^t is the vector of the bus node phase angles for buses 2 to nb at a given time period t . The angle at the slack bus (number 1) is zero, and is therefore eliminated from the formulation.
- G^t is the $ng \times 1$ vector of generation at a given time period t .
- S^t is the $ns \times 1$ vector of power flow from the storage units at a given time period t .
- P_w^t is the $nw \times 1$ vector of generation from wind turbines at a given time period t .
- P_d^t is the $nd \times 1$ vector of the loads at a given time period t .
- $I_1, I_2, I_3,$ and I_4 are matrices that respectively map the vectors $G^t, S^t, P_w^t,$ and P_d^t into $(nb - 1) \times 1$ vectors. The nonzero elements of these vectors match to connection at one of the nb buses, except for the slack bus.

$$B_L \theta^t - F^t = 0, \quad t = 1, \dots, T \quad (4.3)$$

- B_L is the line admittance matrix of the bus system, with column 1 corresponding to the slack bus eliminated.
- F^t is the vector of the line power flows at a given time period t .

$$E_i^t - \Delta t \times S_i^t = E_i^{t+1}, \quad i = 1, \dots, ns, \quad t = 1, \dots, T - 1 \quad (4.4)$$

- S_i is the power directed from the storage unit i into the bus.
- E_i^t is the energy stored in unit i at a given time period t .
- Δt is the length of every time period (for example, it is set to 1 if the problem is to be studied on an hourly basis).

$$R_{down} \leq G_i^t - G_i^{t-1} \leq R_{up}, \quad i = 1, \dots, ng, \quad t = 1, \dots, T \quad (4.5)$$

- R_{down} and R_{up} correspond respectively to the lower and upper limits of the generator ramp rates.

Since the lower and upper bounds of the variables are of primary concern, the following is added to the problem formulation (4.6)-(4.9):

$$G_i^{min} \leq G_i^t \leq G_i^{max}, \quad i = 1, \dots, ng, \quad t = 1, \dots, T \quad (4.6)$$

$$F_{ij}^{min} \leq F_{ij}^t \leq F_{ij}^{max}, \quad i = 1, \dots, nb, \quad j = 1, \dots, nb, \quad i \neq j, \quad t = 1, \dots, T \quad (4.7)$$

$$S_i^{min} \leq S_i^t \leq S_i^{max}, \quad i = 1, \dots, ns, \quad t = 1, \dots, T \quad (4.8)$$

$$E_i^{min} \leq E_i^t \leq E_i^{max}, \quad i = 1, \dots, ns, \quad t = 1, \dots, T \quad (4.9)$$

If the phase angles are to be removed from the problem setup, then the vector of the phase angles is obtained from (4.2), and then replaced in (4.3) by doing a variable substitution as explained below:

- From (4.2): $\theta^t = B^{-1} (I_3 P_w^t - I_4 P_d^t + I_1 G^t + I_2 S^t)$

B^{-1} , the inverse of B , must be calculated after removing the first row of B corresponding to the slack bus.

- Replace θ^t in (4.3).

The following equation is obtained:

$$B_L B^{-1} I_1 G^t + B_L B^{-1} I_2 S^t - F^t = -B_L B^{-1} (I_3 P_w^t - I_4 P_d^t) \quad (4.10)$$

Knowing that F^{max} is the vector of maximum line power flows, equation (4.10) is equivalent to writing the following power flow limit equation replacing equations (4.2), (4.3), and (4.7) [18]:

$$|L \times (I_1 G^t + I_2 S^t + I_3 P_w^t - I_4 P_d^t)| \leq F^{max}, \quad t = 1, \dots, T \quad (4.11)$$

Given that the number of lines of the power system is represented by nl , $L = B_L B^{-1}$ is an $nl \times (nb - 1)$ matrix of power transfer distribution factors.

A power balance constraint equation is added such that the total input power to the system must be equal to the total output power. This is shown in (4.12).

$$\sum_{i=1}^{ng} G_i^t + \sum_{i=1}^{ns} S_i^t = \sum_{i=1}^{nw} (P_{wi}^t) + \sum_{i=1}^{nd} (P_{di}^t), \quad t = 1, \dots, T \quad (4.12)$$

The basic OPF problem without the RES uncertainty, given by the objective (4.1) and subject to (4.4)-(4.6), (4.8), (4.9), (4.11) and (4.12), can be solved via quadratic programming.

B. Demonstration Example

As an example, a 4-Bus System is considered, where:

- a conventional generator (G_1) is connected at bus-1;
- a conventional generator (G_2) and a load (P_{d2}) are connected at bus-2;
- a wind turbine (P_{w3}) and a storage unit (S_3) having a capacity E_3 are connected at bus-3;
- a wind turbine (P_{w4}) and a load (P_{d4}) are connected at bus-4.

The diagram of the system is represented in Figure 4-1.

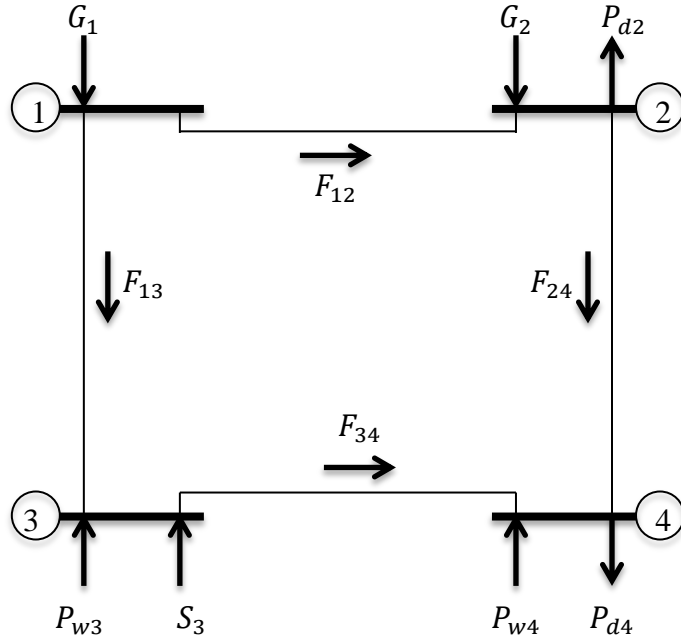


Figure 4-1: 4-bus system

For this system, the objective function is given by:

$$\text{minimize } \sum_{t=1}^T \sum_{i=1}^2 c_{i2}^t (G_i^t)^2 + c_{i1}^t G_i^t \quad (4.13)$$

Equation (4.13) is equivalent to writing the following:

$$\text{minimize } \sum_{t=1}^T c_{12}^t (G_1^t)^2 + c_{11}^t G_1^t + c_{22}^t (G_2^t)^2 + c_{21}^t G_2^t \quad (4.14)$$

The constraints are given by the following set of equations:

- Power flow limit constraints:

$$|L_{11}G_2^t + L_{12}S_3^t + L_{12}P_{w3}^t + L_{13}P_{w4}^t - L_{11}P_{d2}^t - L_{13}P_{d4}^t| \leq F_{12}^{max}, \quad t = 1, \dots, T \quad (4.15)$$

$$|L_{21}G_2^t + L_{22}S_3^t + L_{22}P_{w3}^t + L_{23}P_{w4}^t - L_{21}P_{d2}^t - L_{23}P_{d4}^t| \leq F_{24}^{max}, \quad t = 1, \dots, T \quad (4.16)$$

$$|L_{31}G_2^t + L_{32}S_3^t + L_{32}P_{w3}^t + L_{33}P_{w4}^t - L_{31}P_{d2}^t - L_{33}P_{d4}^t| \leq F_{34}^{max}, \quad t = 1, \dots, T \quad (4.17)$$

$$|L_{41}G_2^t + L_{42}S_3^t + L_{42}P_{w3}^t + L_{43}P_{w4}^t - L_{41}P_{d2}^t - L_{43}P_{d4}^t| \leq F_{13}^{max}, \quad t = 1, \dots, T \quad (4.18)$$

- $E_3^t - \Delta t \times S_3^t = E_3^{t+1}, \quad t = 1, \dots, T - 1 \quad (4.19)$

- Generator ramp rate constraints:

$$R_{down} \leq G_1^t - G_1^{t-1} \leq R_{up}, \quad t = 1, \dots, T \quad (4.20)$$

$$R_{down} \leq G_2^t - G_2^{t-1} \leq R_{up}, \quad t = 1, \dots, T \quad (4.21)$$

- Lower and upper bounds constraints:

$$G_1^{min} \leq G_1^t \leq G_1^{max}, \quad t = 1, \dots, T \quad (4.22)$$

$$G_2^{min} \leq G_2^t \leq G_2^{max}, \quad t = 1, \dots, T \quad (4.23)$$

$$S_3^{min} \leq S_3^t \leq S_3^{max}, \quad t = 1, \dots, T \quad (4.24)$$

$$E_3^{min} \leq E_3^t \leq E_3^{max}, \quad t = 1, \dots, T \quad (4.25)$$

- Power balance constraint:

$$G_1^t + G_2^t + S_3^t = -P_{w3}^t - P_{w4}^t + P_{d2}^t + P_{d4}^t, \quad t = 1, \dots, T \quad (4.26)$$

CHAPTER V

APPLYING ROBUST OPTIMIZATION TO THE OPF PROBLEM

A. Overview

It is often insufficient to find high-quality solutions for many problems, but the solutions have to be robust as well; this means that the solution quality does not completely weaken even if a slight change of the parameters involved in the problem occurs. In other words, some deviations from the main solution are accepted without a total loss in the quality of the problem [27].

Robust optimization deals with problems in which a certain measure of robustness is pursued against uncertainty that can be represented as a deterministic variability in the parameters' value of the problem.

In the first part of the chapter, the problem is formulated by taking into account the uncertainty of the output power from wind turbines; thus, the output power can fluctuate in a pre-defined interval. In the second part, an affinely adjustable robust OPF is applied to the problem formulation. Then, a demonstration example is included in which the objective function and the constraints are written explicitly.

B. Problem Formulation With RES Uncertainty

In order to take the uncertainty of the output power from wind turbines into consideration, a vector ζ is defined, which is an $n_w \times 1$ vector belonging to the uncertainty set $[\zeta^{min}, \zeta^{max}]$ of the wind turbines output variation. This is illustrated in equation (5.1):

$$P_{wi(actual)}^t = P_{wi}^t + \zeta_i^t, \quad i = 1, \dots, nw, \quad t = 1, \dots, T \quad (5.1)$$

- $P_{wi(actual)}^t$ is the actual wind output power from wind generator i for time period t .
- P_{wi}^t is the wind power output forecast from wind generator i for time period t .
- ζ_i^t is the wind power forecast error from wind generator i for time period t .

The power generation consists of the base-point value $G_{i(base)}$ that is the output corresponding to nominal conditions, and the generation changes corresponding to wind turbines output fluctuations [18]. Therefore, the following formula is established for every time period t (5.2):

$$G_i^t = G_{i(base)}^t - \beta_i^t \times \sum_{j=1}^{nw} \zeta_j^t, \quad i = 1, \dots, ng, \quad t = 1, \dots, T \quad (5.2)$$

As shown in (5.2), β_i^t represents the participation factor of generation unit i at t , which is the rate of change of the generator output corresponding to the change in total controllable generation. Therefore, for every time interval, (4.12) becomes:

$$\sum_{i=1}^{ng} G_{i(base)}^t + \sum_{i=1}^{ns} S_i^t = \sum_{i=1}^{nw} P_{wi}^t + \sum_{i=1}^{nd} P_{di}^t, \quad t = 1, \dots, T \quad (5.3)$$

Under uncertainty, the generation levels in (4.5) and (4.6) are considered a function of the base-point generation as well as the participation factors as shown in (5.2).

The line power flow constraint is limited by F^{max} and given by (5.4) for every time period:

$$|L \times (I_1 G^t + I_2 S^t + I_3 (P_w^t + \zeta^t) - I_4 P_d^t)| \leq F^{max}, \quad t = 1, \dots, T \quad (5.4)$$

As far as the cost function of the problem (4.1) is concerned, it is expressed in terms of base-point generation as shown in (5.5):

$$\sum_{t=1}^T \sum_{i=1}^{ng} c_{i2}^t (G_{i(base)}^t)^2 + c_{i1}^t G_{i(base)}^t \quad (5.5)$$

C. Affinely Adjustable Robust OPF

Let $u^t = [G_{base}^t ; S^t]$ denote the vector of non-adjustable variables and v^t the vector of adjustable variables. v^t is affinely related to the uncertainty vector ζ^t that contains the elements of the wind power generation uncertain data at different time intervals as shown in (5.6):

$$v^t = W\zeta^t, \quad \text{where } W \text{ is an } ng \times nw \text{ matrix of ones.} \quad (5.6)$$

The OPF problem for a given $\zeta^t \in [\zeta^{t \min}, \zeta^{t \max}]$ can be written in terms of u^t and v^t as follows [18]:

$$\text{minimize}_{u,v} \sum_{t=1}^T \sum_{i=1}^{ng} c_{i2}^t (G_{i(base)}^t)^2 + c_{i1}^t G_{i(base)}^t \quad (5.7)$$

$$\text{subject to } \sum_{i=1}^{ng+ns} u_i^t = \sum_{i=1}^{nw} -P_{wi}^t + \sum_{i=1}^{nd} P_{di}^t, \quad t = 1, \dots, T \quad (5.8)$$

$$\text{and } Uu^t + V^t v^t \leq A\zeta^t + b^t, \quad t = 1, \dots, T. \quad (5.9)$$

Knowing that I_G and I_S are the identity matrices of sizes $ng \times ng$ and $ns \times ns$ respectively, and $diag\{\beta\}$ is a diagonal matrix with elements β_i , the matrices U , V^t , A , and the vector b^t are defined as follows (for every time period) [18]:

$$U = \begin{bmatrix} I_G & 0_{(ng \times ns)} \\ -I_G & 0_{(ng \times ns)} \\ 0_{(ns \times ng)} & I_S \\ 0_{(ns \times ng)} & -I_S \\ L \times I_1 & L \times I_2 \\ -L \times I_1 & -L \times I_2 \end{bmatrix}, \quad V^t = \begin{bmatrix} -diag\{\beta^t\} \\ diag\{\beta^t\} \\ 0_{(ns \times ng)} \\ 0_{(ns \times ng)} \\ -L \times I_1 \times diag\{\beta^t\} \\ L \times I_1 \times diag\{\beta^t\} \end{bmatrix}, \quad t = 1, \dots, T \quad (5.10)$$

$$A = \begin{bmatrix} 0_{(ng \times nw)} \\ 0_{(ng \times nw)} \\ 0_{(ns \times nw)} \\ 0_{(ns \times nw)} \\ -L \times I_3 \\ L \times I_3 \end{bmatrix}, \quad b^t = \begin{bmatrix} G_{max} \\ -G_{min} \\ S_{max} \\ -S_{min} \\ F_{max} + L \times I_4 \times P_d^t - L \times I_3 \times P_w^t \\ F_{max} - L \times I_4 \times P_d^t + L \times I_3 \times P_w^t \end{bmatrix}, \quad t = 1, \dots, T. \quad (5.11)$$

The AAROPF aims to find u^t that minimizes the objective function in (5.7) subject to the equality and inequality constraints represented in (5.8) and (5.9) respectively. For every row i of the constraint in (5.9), and given (5.6), the last condition can be written as:

$$U_i u^t - b_i^t + \max_{\zeta^t \in [\zeta^{t \min}, \zeta^{t \max}]} (V_i^t W - A_i) \zeta^t \leq 0, \quad t = 1, \dots, T. \quad (5.12)$$

where, $\max_{\zeta^t \in [\zeta^{t \min}, \zeta^{t \max}]} (V_i^t W - A_i) \zeta^t$ can be expressed as:

$$\sum_j \max([V_i^t W - A_i]_j, 0) \zeta_j^{t \max} + \sum_j \min([V_i^t W - A_i]_j, 0) \zeta_j^{t \min} \quad (5.13)$$

By making use of row vectors of positive/negative slack variables z_i^T / \bar{z}_i^T in (5.13) and knowing that m is the number of rows in the data matrices/vectors U, V^t, A, b^t , the AAROPF is written as a quadratic program represented in (5.7) and subject to (5.8) and the following equations:

$$U_i u^t - b_i^t + (\zeta^{t \max})^T z_i + (\zeta^{t \min})^T \bar{z}_i \leq 0, \quad i = 1, \dots, m, \quad t = 1, \dots, T \quad (5.14)$$

$$z_i \geq 0, \quad z_i^T \geq V_i^t W - A^i, \quad i = 1, \dots, m, \quad t = 1, \dots, T \quad (5.15)$$

$$\bar{z}_i \leq 0, \quad \bar{z}_i^T \leq V_i^t W - A^i, \quad i = 1, \dots, m, \quad t = 1, \dots, T. \quad (5.16)$$

The generator participation factors β_i^t that are present in the matrix V^t can be treated as either fixed parameters or variables. However, in both cases, the linearity of the AAROPF constraints is preserved. In case they are treated as variables, their sum is set to one as shown in (5.17):

$$\sum_{i=1}^{ng} \beta_i^t = 1, \quad t = 1, \dots, T \quad (5.17)$$

Quadratic programming is used to solve the AAROPF, which is given by (5.7) subject to (5.8) and (5.14)-(5.17).

D. Demonstration Example

The example shown in the previous chapter is now considered; however, the uncertainty of the wind power generation is taken into consideration, and AAROPF is applied to the problem.

For this system, the objective function is given by:

$$\text{minimize } \sum_{t=1}^T c_{12}^t (G_{1(base)}^t)^2 + c_{11}^t G_{1(base)}^t + c_{22}^t (G_{2(base)}^t)^2 + c_{21}^t G_{2(base)}^t \quad (5.18)$$

The constraints are given by the following equations:

- Power flow limit constraints:

$$\left| \begin{array}{c} L_{11}G_{2(base)}^t + L_{12}S_3^t + L_{12}P_{w3}^t + L_{13}P_{w4}^t - L_{11}\beta_2^t(\zeta_3^t + \zeta_4^t) + L_{12}\zeta_3^t + L_{13}\zeta_4^t \\ -L_{11}P_{d2}^t - L_{13}P_{d4}^t \end{array} \right| \leq F_{12}^{max}, \quad t = 1, \dots, T \quad (5.19)$$

$$\left| \begin{array}{c} L_{21}G_{2(base)}^t + L_{22}S_3^t + L_{22}P_{w3}^t + L_{23}P_{w4}^t - L_{21}\beta_2^t(\zeta_3^t + \zeta_4^t) + L_{22}\zeta_3^t + L_{23}\zeta_4^t \\ -L_{21}P_{d2}^t - L_{23}P_{d4}^t \end{array} \right| \leq F_{24}^{max}, \quad t = 1, \dots, T \quad (5.20)$$

$$\left| \begin{array}{c} L_{31}G_{2(base)}^t + L_{32}S_3^t + L_{32}P_{w3}^t + L_{33}P_{w4}^t - L_{31}\beta_2^t(\zeta_3^t + \zeta_4^t) + L_{32}\zeta_3^t + L_{33}\zeta_4^t \\ -L_{31}P_{d2}^t - L_{33}P_{d4}^t \end{array} \right| \leq F_{34}^{max}, \quad t = 1, \dots, T \quad (5.21)$$

$$\left| \begin{array}{c} L_{41}G_{2(base)}^t + L_{42}S_3^t + L_{42}P_{w3}^t + L_{43}P_{w4}^t - L_{41}\beta_2^t(\zeta_3^t + \zeta_4^t) + L_{42}\zeta_3^t + L_{43}\zeta_4^t \\ -L_{41}P_{d2}^t - L_{43}P_{d4}^t \end{array} \right| \leq F_{13}^{max}, \quad t = 1, \dots, T \quad (5.22)$$

- $E_3^t - \Delta t \times S_3^t = E_3^{t+1}, \quad t = 1, \dots, T - 1 \quad (5.23)$

- Generator ramp rate constraints:

$$R_{down} \leq G_{1(base)}^t - \beta_1^t(\zeta_3^t + \zeta_4^t) - G_{1(base)}^{t-1} + \beta_1^{t-1}(\zeta_3^{t-1} + \zeta_4^{t-1}) \leq R_{up},$$

$$t = 1, \dots, T \quad (5.24)$$

$$R_{down} \leq G_{2(base)}^t - \beta_2^t(\zeta_3^t + \zeta_4^t) - G_{2(base)}^{t-1} + \beta_2^{t-1}(\zeta_3^{t-1} + \zeta_4^{t-1}) \leq R_{up},$$

$$t = 1, \dots, T \quad (5.25)$$

- Lower and upper bounds constraints:

$$G_1^{min} \leq G_{1(base)}^t - \beta_1^t(\zeta_3^t + \zeta_4^t) \leq G_1^{max}, \quad t = 1, \dots, T \quad (5.26)$$

$$G_2^{min} \leq G_{2(base)}^t - \beta_2^t(\zeta_3^t + \zeta_4^t) \leq G_2^{max}, \quad t = 1, \dots, T \quad (5.27)$$

$$S_3^{min} \leq S_3^t \leq S_3^{max}, \quad t = 1, \dots, T \quad (5.28)$$

$$E_3^{min} \leq E_3^t \leq E_3^{max}, \quad t = 1, \dots, T \quad (5.29)$$

- Power balance constraint:

$$G_{1(base)}^t + G_{2(base)}^t + S_3^t = -P_{w3}^t - P_{w4}^t + P_{d2}^t + P_{d4}^t, \quad t = 1, \dots, T \quad (5.30)$$

CHAPTER VI

SIMULATION RESULTS

In the first part of this chapter, two mathematical models used for the prediction of wind power are shown and explained. In the second part, the results of the simulations performed, demonstrated in graphical and tabular forms, are interpreted and analyzed.

A. Wind Power Prediction Models

In [28], a standardized protocol is proposed for the evaluation of short-term (up to 48 hours ahead) wind power prediction systems. According to this reference, the “reference model” that is used for wind power prediction is the Persistence model; this model states that the future wind predicted production made at time origin t , and represented by $\hat{P}_p(t + k|t)$ is the same as the last measured power value represented by $P(t)$, where k is the prediction time-step ($k = 1, 2, \dots, k_{max}$). This is shown in the following equation [28]:

$$\hat{P}_p(t + k|t) = P(t) \quad (6.1)$$

The prediction error is defined as the difference between the measured value $P(t + k)$ and the predicted one $\hat{P}(t + k|t)$ as shown below [28]:

$$e(t + k|t) = P(t + k) - \hat{P}(t + k|t) \quad (6.2)$$

One of the basic criteria to illustrate a predictor’s performance is using the mean absolute error (*MAE*) knowing that N is the number of data points used for the model

evaluation [28]. This is given by:

$$MAE(k) = \frac{1}{N} \sum_{t=1}^N |e(t+k|t)| \quad (6.3)$$

In order to produce results independent of wind farm sizes, it is possible to normalize this criterion by the average measured wind power production (P) over the whole forecast period. Thus, the normalized mean absolute error ($NMAE$) is used and given by [28]:

$$NMAE(k) = \frac{MAE(k)}{\sum_{t=1}^N P(t)} = \frac{\sum_{t=1}^N |e(t+k|t)|}{\sum_{t=1}^N P(t)} \quad (6.4)$$

Reference [28] evaluates the performances of the Persistence model as well as a state-of-the-art artificial intelligence based forecasting approach referred to as an “advanced” approach based on the $NMAE$ criterion for four different wind farm sites. It is shown that the $NMAE$ increases linearly (from 10% for $k = 1$) in the “Advanced” forecasting approach; however, in the Persistence forecasting model, it increases in the form of a power curve (from 5% for $k = 1$) having the equation:

$$NMAE(k) = 0.05 \times k^x, \quad k = 1, \dots, T, \quad x \text{ is a real parameter} \quad (6.5)$$

For the simulations, three cases in the “Advanced” forecasting approach are taken into consideration over a 24-hour study horizon, where:

- $NMAE$ increases from 10% to 15% in the first case;
- $NMAE$ increases from 10% to 20% in the second case;
- $NMAE$ increases from 10% to 25% in the third case.

The three cases are shown in Figure 6-1.

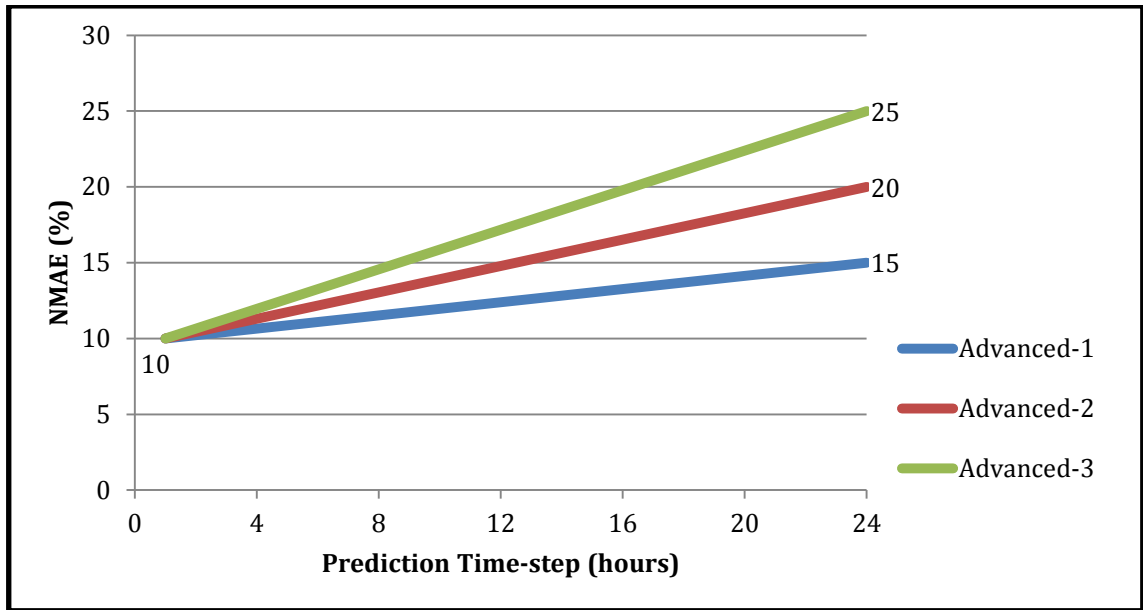


Figure 6-1: Variation of the *NMAE* in the “Advanced” approach for the three cases

In addition, five cases in the Persistence forecasting model are taken into consideration over a 24-hour study horizon, where:

- *NMAE* increases from 5% to 20% in the first case;
- *NMAE* increases from 5% to 30% in the second case;
- *NMAE* increases from 5% to 40% in the third case;
- *NMAE* increases from 5% to 50% in the fourth case;
- *NMAE* increases from 5% to 60% in the fifth case.

The five cases are shown in Figure 6-2.

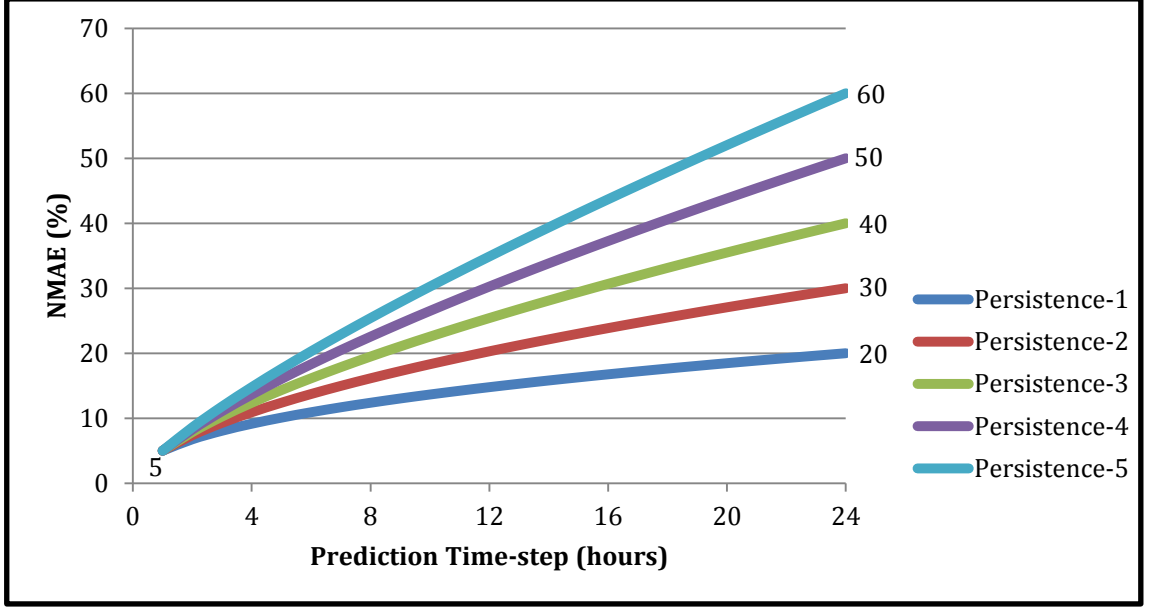


Figure 6-2: Variation of the $NMAE$ in the Persistence model for the five cases

The values of $\zeta^{t max}$ and $\zeta^{t min}$ are calculated using the equations below:

$$\zeta^{t max} = \frac{NMAE^t}{100} \times P_w^t, \quad t = 1, \dots, T \quad (6.6)$$

$$\zeta^{t min} = -\frac{NMAE^t}{100} \times P_w^t, \quad t = 1, \dots, T \quad (6.7)$$

B. Numerical Results

The AAROPF problem formulation was programmed in MATLAB, and the quadratic program was solved using CPLEX [29]. The simulations were carried out on an Intel Core i7 processor running at 2 GHz with 4 GB DDR3 of memory.

The AAROPF was tested on the IEEE 14-bus and the IEEE 118-bus networks whose data sets are given with the distribution files of MATPOWER [30], and modified according to [31]. For the IEEE 14-bus network, there are two wind farms, with each having a forecasted power output of 40 MW, connected at nodes 2 and 3 respectively.

On the other hand, the IEEE 118-bus network has five wind farms, with a power

forecast of 200 MW for each, connected at nodes 16, 37, 48, 75, and 83 respectively. In addition, storage units, with each having a capacity of 32 MWh, are connected respectively at every node of the 14-bus and 118-bus networks [6]. The maximum and minimum discharging/charging power limits are respectively: $S_i^{max} = 8MW$ and $S_i^{min} = -8MW$.

The non-adjustable variables, the CPLEX solution time, and the total base generation cost were computed for all the cases of the “Advanced” forecasting approach and the Persistence forecasting model by taking into consideration two situations: 1) by fixing the participation factors using equation (6.8) [18], and 2) by allowing the program to automatically choose the participation factors that are treated as variables:

$$\beta_i^t = \frac{1/c_{i2}^t}{\sum_{j=1}^{ng} 1/c_{j2}^t}, \quad i = 1, \dots, ng, \quad t = 1, \dots, T. \quad (6.8)$$

All the results that will be presented hereafter are based on the second case in the “Advanced” forecasting approach where *NMAE* increases from 10% to 20% over the 24-hour study horizon, and the first case in the Persistence forecasting model where *NMAE* increases from 5% to 20%. For all other cases, the results vary similarly.

1. Results for the IEEE 14-Bus Network

a. “Advanced” Forecasting Approach

i. Fixed Participation Factors

For this case, the variations of the total base generation, total storage power, total load, and total wind power are shown in Figure 6-3.

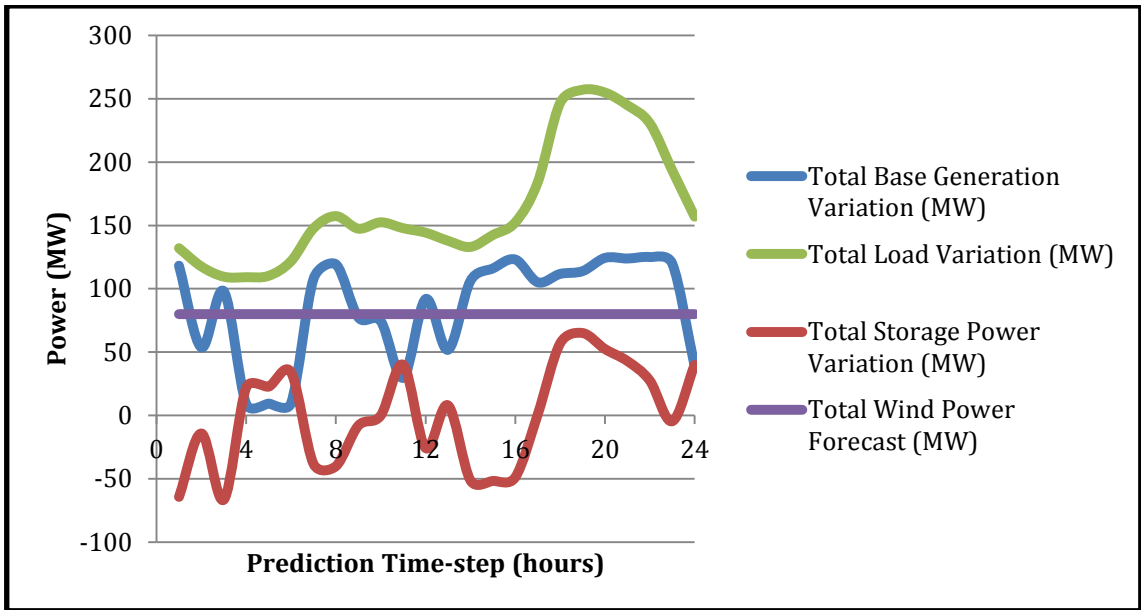


Figure 6-3: Total input and output power of the system for part a.i.

The variation of the total energy stored is shown in Figure 6-4.

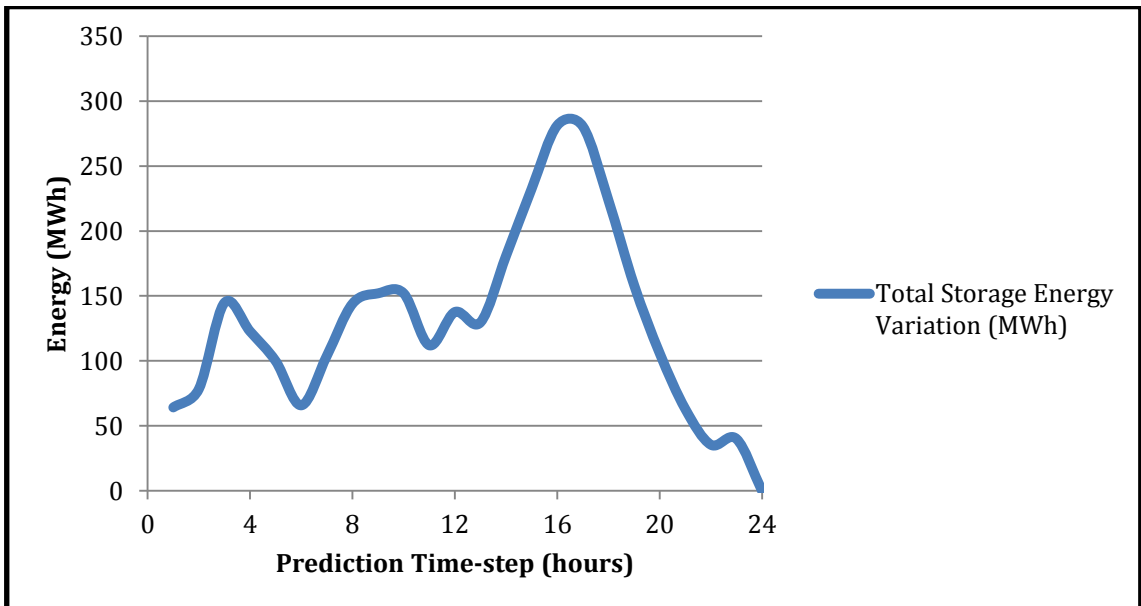


Figure 6-4: Total storage energy variation of the system for part a.i.

ii. Variable Participation Factors

For this case, the variations of the total base generation, total storage power, total load, and total wind power are shown in Figure 6-5.

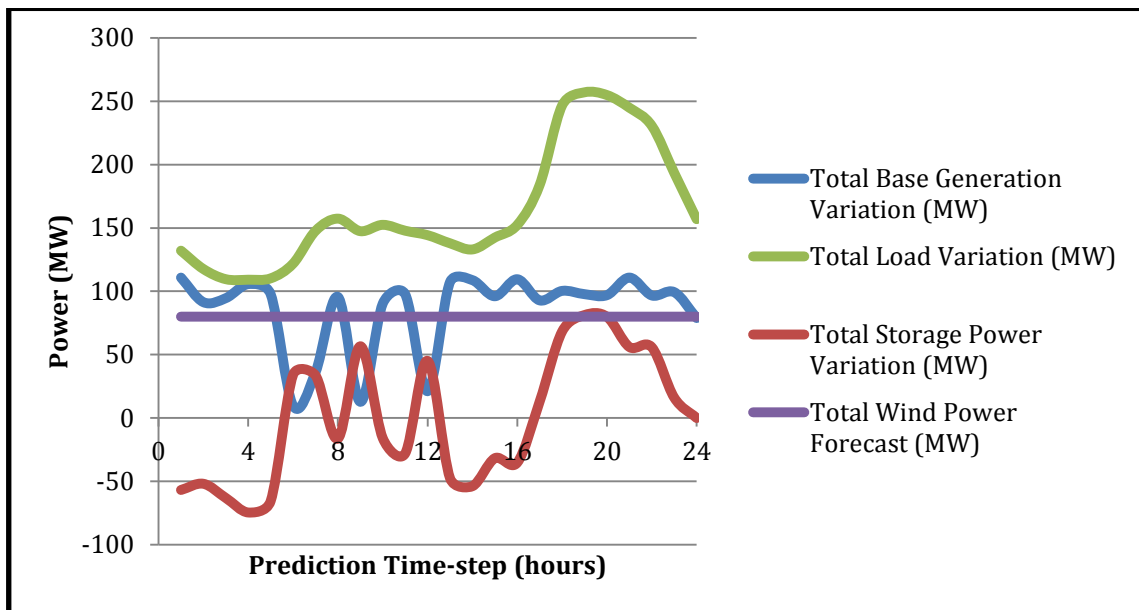


Figure 6-5: Total input and output power of the system for part a.ii.

The variation of the total energy stored is shown in Figure 6-6.

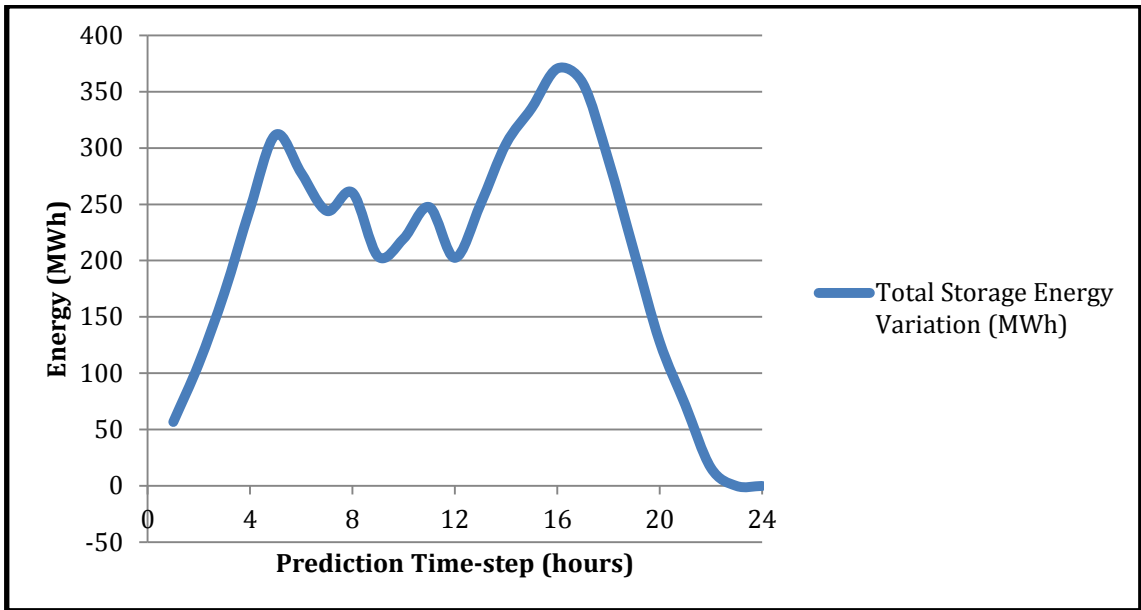


Figure 6-6: Total storage energy variation of the system for part a.ii.

b. Persistence Forecasting Model

i. Fixed Participation Factors

For this case, the variations of the total base generation, total storage power, total load, and total wind power are shown in Figure 6-7.

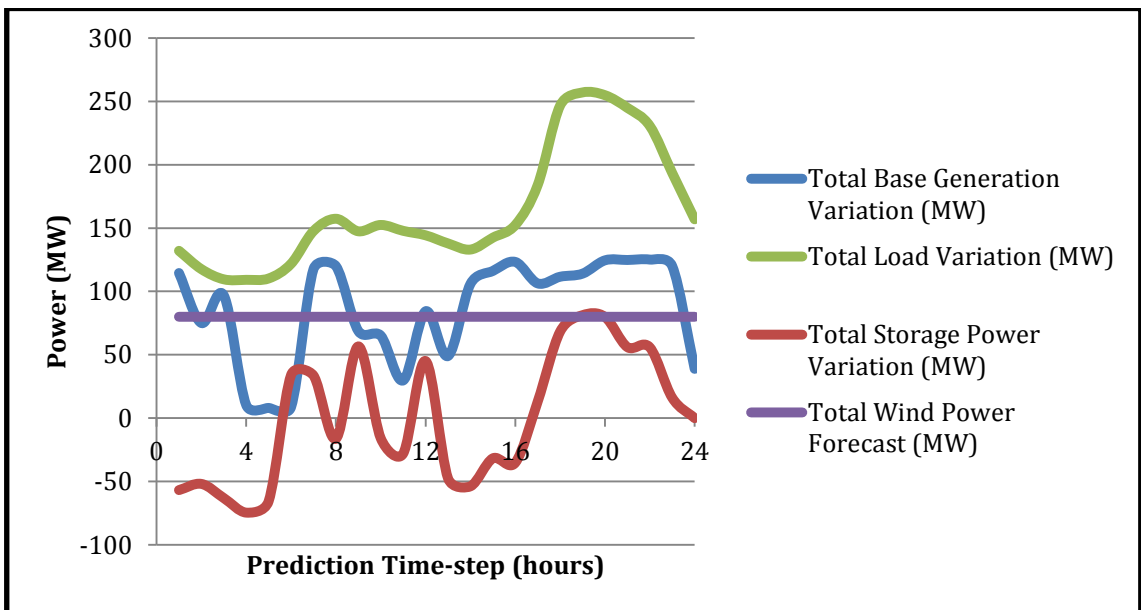


Figure 6-7: Total input and output power of the system for part b.i.

The variation of the total energy stored is shown in Figure 6-8.

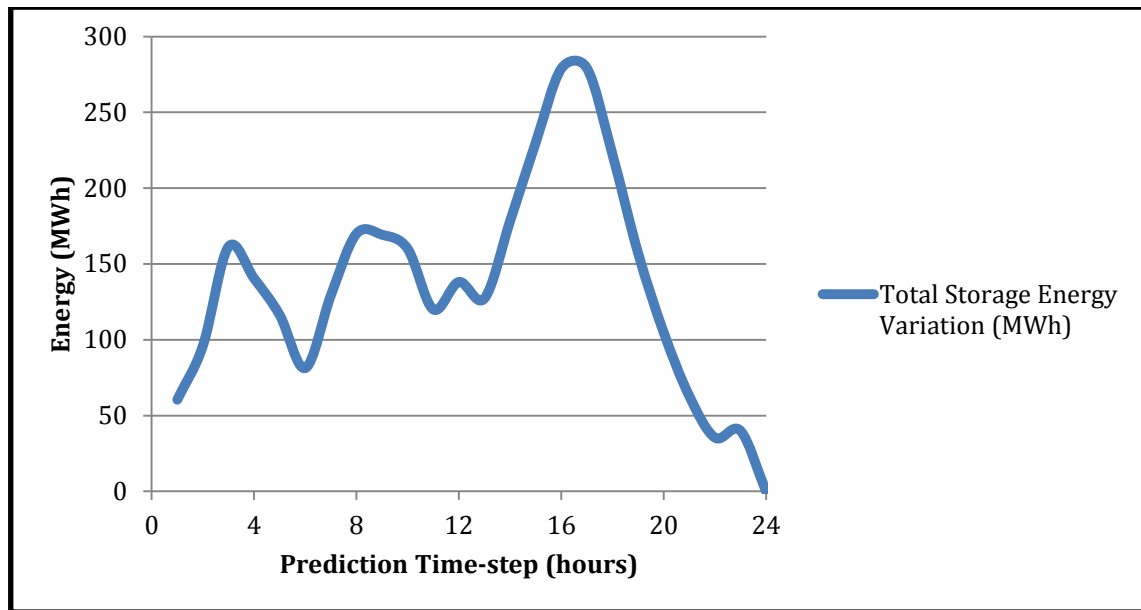


Figure 6-8: Total storage energy variation of the system for part b.i.

ii. Variable Participation Factors

For this case, the variations of the total base generation, total storage power, total load, and total wind power are shown in Figure 6-9.

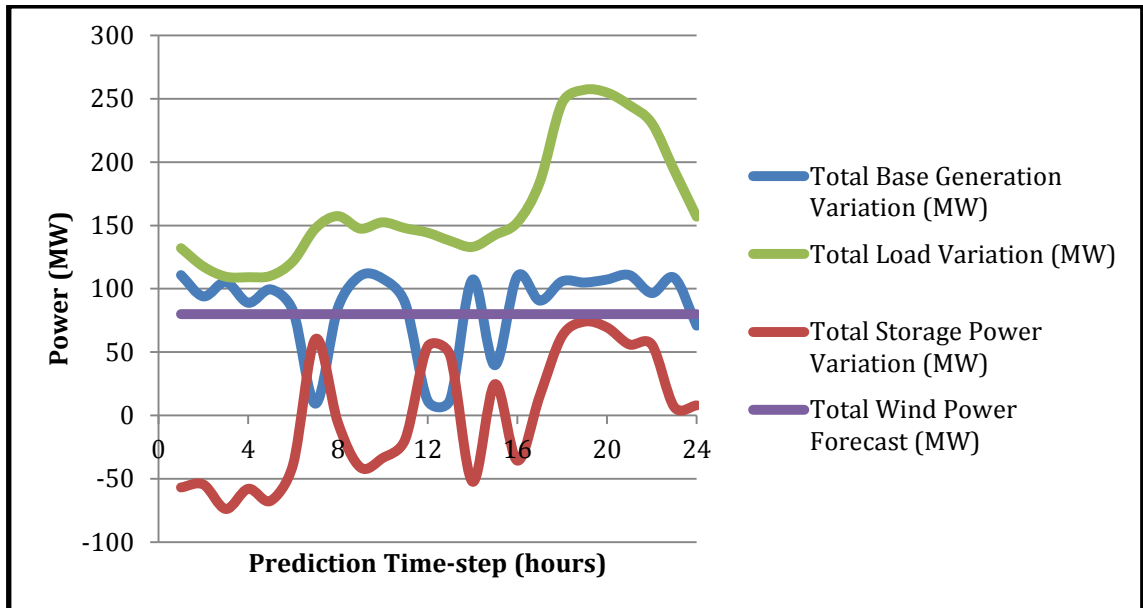


Figure 6-9: Total input and output power of the system for part b.ii.

The variation of the total energy stored is shown in Figure 6-10.

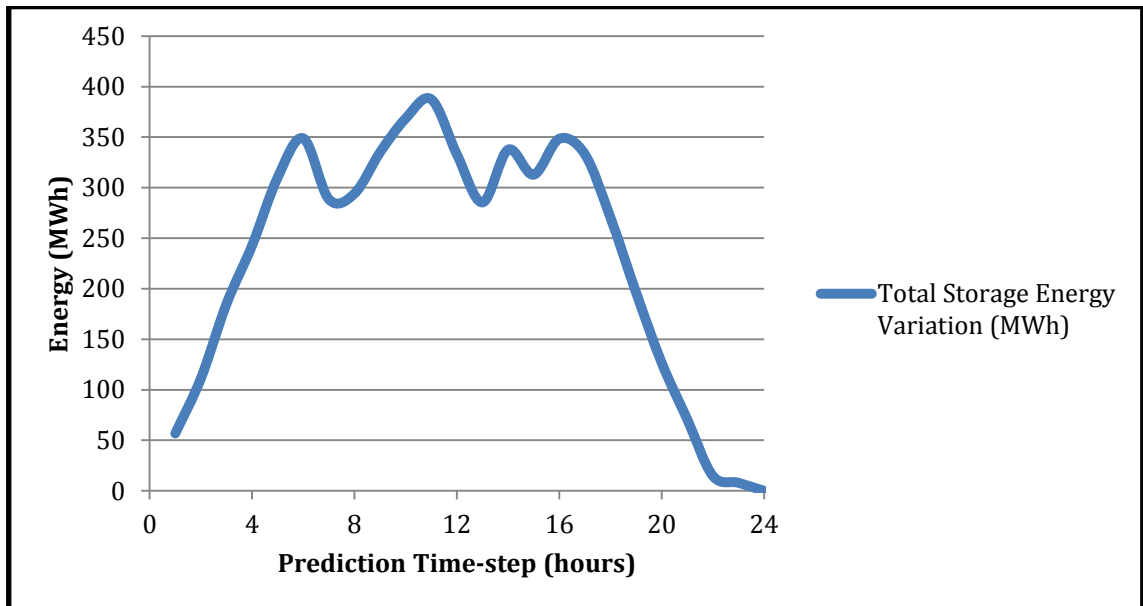


Figure 6-10: Total storage energy variation of the system for part b.ii.

As shown in Figures 6-3 to 6-10, the storage units initially start charging up to a certain limit, and thus, the total storage increases. When the total base generation of the network reaches a minimum value (between periods 4 and 8 for instance), the total storage energy decreases implying that the units are discharging accordingly to supply the total load. In addition, the total energy stored increases as the total base generation increases in order for the units to feed the total load in later periods when there is a decrease in total generation. When the peak load is reached (after 19 hours), the total network storage decreases drastically (the units start discharging) and the total base generation reaches a maximum value. On the other hand, when the total load is at its minimum value, most of the total input power comes from the generators. Thus, the storage units charge up to a certain limit, and the total energy stored increases.

The simulation results show that all the storage units, connected respectively at every node of the 14-bus network, are active. In other words, they either charge or discharge over the 24-hour study horizon.

The plots present in Figures 6-3, 6-5, 6-7, and 6-9 verify the balance between the supply and the demand as illustrated in equation (5.8).

2. Results for the IEEE 118-Bus Network

Similar variations of the total base generation, total storage power, total load, and total wind power are obtained after running the program for the 118-bus network. For the case of the “Advanced” forecasting approach (where $NMAE$ increases from 10% to 20% over the 24-hour study horizon) with fixed participation factors, the results are shown in Figure 6-11.

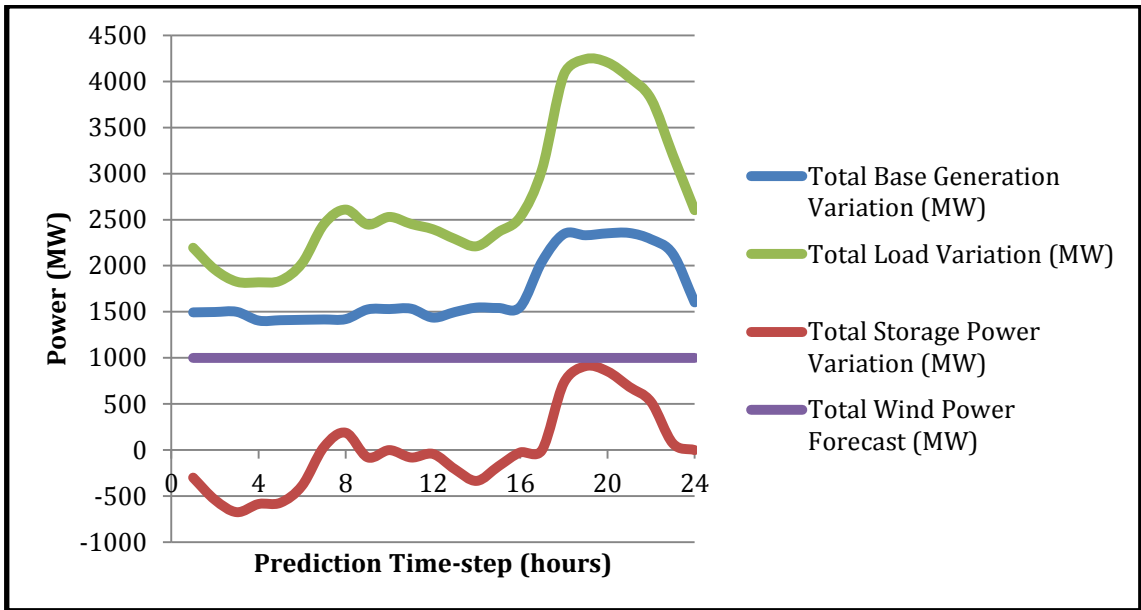


Figure 6-11: Total input and output power of the 118-bus system

The variation of the total energy stored is shown in Figure 6-12.

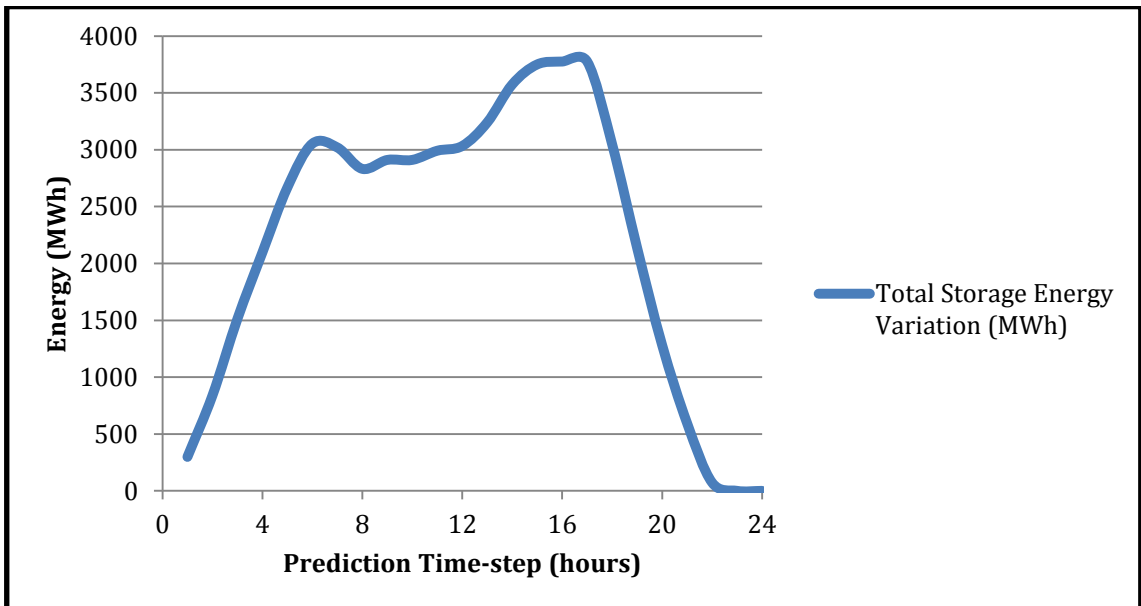


Figure 6-12: Total storage energy variation of the 118-bus system

Similar interpretation of the results applies as in the case of the 14-bus network. In addition, all the storage units, connected respectively at all nodes of the 118-bus

network, are active over the 24-hour study horizon.

The CPLEX solution time and the total base generation cost are tabulated (Tables 6.1 and 6.2) for the 14-bus and 118-bus networks without taking uncertainty into consideration, and then by taking into account all the analyzed cases of the “Advanced” forecasting approach and the Persistence forecasting model and fixing or varying the participation factors.

Table 6.1: CPLEX solution time (seconds) for all the cases studied

Studied Cases	IEEE 14-bus		IEEE 118-bus	
	Fixed β	Variable β	Fixed β	Variable β
Without Uncertainty	0.7	0.1	2.3	3.3
Advanced-1	0.4	0.2	2.0	36.6
Advanced-2	0.1	0.2	5.0	81.5
Advanced-3	0.1	0.1	1.7	73.9
Persistence-1	0.1	0.2	3.9	60.8
Persistence-2	0.05	0.2	1.9	73.0
Persistence-3	0.1	0.2	1.9	194.5
Persistence-4	0.2	0.2	1.7	198.4
Persistence-5	0.1	0.2	1.9	192.8

Table 6.2: Total base generation cost (dollars) for all the cases studied

Studied Cases	IEEE 14-bus		IEEE 118-bus	
	Fixed β	Variable β	Fixed β	Variable β
Without Uncertainty	50994	50994	1023090	1023090
Advanced-1	54439	50994	1057844	1023090
Advanced-2	55128	50994	1064406	1023090
Advanced-3	55817	50994	1071039	1023090
Persistence-1	54934	50994	1062017	1023090
Persistence-2	56443	50994	1076796	1023090
Persistence-3	57879	51055	1091099	1023090
Persistence-4	59265	51207	1105316	1023090
Persistence-5	60613	51381	1120238	1023090

According to Table 6.1, CPLEX generally took more time to execute the results of both bus networks having variable participation factors for the connected generators than those having fixed participation factors. For instance, for the second case of the “advanced” forecasting approach, where $NMAE$ increases from 10% to 20% over the 24-hour study horizon, CPLEX took about 2 and 16 times the time for the 14-bus and the 118-bus networks respectively. Moreover, for the first case of the Persistence forecasting model, where $NMAE$ increases from 5% to 20%, CPLEX also took about 2 and 16 times the time for both networks respectively.

Table 6.2 shows that the total base generation cost for both networks having variable participation factors is less than those having fixed participation factors. For example, for the second case of the “Advanced” forecasting approach, the percent decrease in the cost is about 8% and 4% for the 14-bus and 118-bus networks respectively.

Table 6.3 shows the percentage increase in cost relative to the cost without uncertainty. It confirms that as the level of uncertainty increases in the “Advanced” forecasting approach as well as in the Persistence forecasting model, the percentage increase in cost relative to the cost without uncertainty increases for networks with the fixed generator participation factors as given in (6.8). However, the percentage increase in cost is nearly 0% for networks with variable participation factors no matter what the level of uncertainty is. This demonstrates the importance of optimizing the participation factors using affinely adjustable robust optimization.

Table 6.3: Percentage increase in cost relative to the cost without uncertainty

Studied Cases	IEEE 14-bus		IEEE 118-bus	
	Fixed β	Variable β	Fixed β	Variable β
Advanced-1	6.8	0.0	3.4	0.0
Advanced-2	8.1	0.0	4.0	0.0
Advanced-3	9.5	0.0	4.7	0.0
Persistence-1	7.7	0.0	3.8	0.0
Persistence-2	10.7	0.0	5.2	0.0
Persistence-3	13.5	0.1	6.6	0.0
Persistence-4	16.2	0.4	8.0	0.0
Persistence-5	18.9	0.8	9.5	0.0

In all the studied cases, a Monte Carlo simulation (MCS) with 10 000 trials shows a 100% success rate; thus, MCS confirms that AAROPF completely immunizes the results against all the variations that are captured by the uncertainty set, and produces optimal and robust solution. The Monte Carlo trials are formed by the RES generation sampled from a uniform distribution over the uncertainty set interval bounds; a trial is considered successful if none of the power flow or generation limits are violated after rescheduling the generation in agreement with the participation factors [18].

CHAPTER VII

CONCLUSION

Optimal power flow with renewable energy and storage integration is a widely researched topic. This thesis presents an AAROPF for networks having wind generation and storage units connected at some nodes over a 24-hour study horizon.

The problem is solved via quadratic programming using CPLEX, and robust optimal solutions are obtained for all the cases studied. The adjustable variables, which are computed through generator participation factors, restore feasibility for all the realizations within the uncertainty set of the wind power output variation. The main results show that the total base generation cost is less for networks having variable generator participation factors than those having fixed participation factors. Moreover, there is a small increase in the base generation cost for increasing levels of uncertainty represented by *NMAE*. The solutions obtained were validated by MCS with 10 000 trials showing a 100% success rate.

AAROPF can be implemented on any bus network over multiple time periods and still produces optimal and robust solutions. As possible future work, the AAROPF problem can take into account the participation factors of the storage units connected at the nodes. In addition, the charging/discharging efficiency for every storage device may be included in the formulation of the problem.

APPENDIX I

IEEE 14-BUS SYSTEM DATA

Table A.1: IEEE 14-bus bus data

bus_i	type	Pd	Qd	Gs	Bs	area	Vm	Va	baseKV	zone	Vmax	Vmin
1	3	0	0	0	0	1	1.06	0	0	1	1.06	0.94
2	2	21.7	12.7	0	0	1	1.045	-4.98	0	1	1.06	0.94
3	2	94.2	19	0	0	1	1.01	-12.72	0	1	1.06	0.94
4	1	47.8	-3.9	0	0	1	1.019	-10.33	0	1	1.06	0.94
5	1	7.6	1.6	0	0	1	1.02	-8.78	0	1	1.06	0.94
6	2	11.2	7.5	0	0	1	1.07	-14.22	0	1	1.06	0.94
7	1	0	0	0	0	1	1.062	-13.37	0	1	1.06	0.94
8	2	0	0	0	0	1	1.09	-13.36	0	1	1.06	0.94
9	1	29.5	16.6	0	19	1	1.056	-14.94	0	1	1.06	0.94
10	1	9	5.8	0	0	1	1.051	-15.1	0	1	1.06	0.94
11	1	3.5	1.8	0	0	1	1.057	-14.79	0	1	1.06	0.94
12	1	6.1	1.6	0	0	1	1.055	-15.07	0	1	1.06	0.94
13	1	13.5	5.8	0	0	1	1.05	-15.16	0	1	1.06	0.94
14	1	14.9	5	0	0	1	1.036	-16.04	0	1	1.06	0.94

Table A.2: IEEE 14-bus generator data

bus	Pg	Qg	Qmax	Qmin	Vg	mBase	status	Pmax	Pmin
1	232.4	-16.9	10	0	1.06	100	1	332.4	0
2	40	42.4	50	-40	1.045	100	1	140	0
3	0	23.4	40	0	1.01	100	1	100	0
6	0	12.2	24	-6	1.07	100	1	100	0
8	0	17.4	24	-6	1.09	100	1	100	0

Table A.3: IEEE 14-bus branch data

fbus	tbus	r	x	b
1	2	0.01938	0.05917	0.0528
1	5	0.05403	0.22304	0.0492
2	3	0.04699	0.19797	0.0438
2	4	0.05811	0.17632	0.034
2	5	0.05695	0.17388	0.0346
3	4	0.06701	0.17103	0.0128
4	5	0.01335	0.04211	0
4	7	0	0.20912	0
4	9	0	0.55618	0
5	6	0	0.25202	0
6	11	0.09498	0.1989	0
6	12	0.12291	0.25581	0
6	13	0.06615	0.13027	0
7	8	0	0.17615	0
7	9	0	0.11001	0
9	10	0.03181	0.0845	0
9	14	0.12711	0.27038	0
10	11	0.08205	0.19207	0
12	13	0.22092	0.19988	0
13	14	0.17093	0.34802	0

Table A.4: IEEE 14-bus generator cost data

bus	c_2	c_1
1	0.0430293	20
2	0.25	20
3	0.01	40
6	0.01	40
8	0.01	40

Table A.5: IEEE 14-bus storage data for every storage unit

max. storage	min. storage	max. storage rate	min. storage rate	initial storage	final storage
32 MWh	0 MWh	8 MW	-8 MW	0	0

APPENDIX II

IEEE 118-BUS SYSTEM DATA

Table A.6: IEEE 118-bus bus data

bus_i	type	Pd	Qd	Gs	Bs	area	Vm	Va	baseKV	zone	Vmax	Vmin
1	2	51	27	0	0	1	0.955	10.67	138	1	1.06	0.94
2	1	20	9	0	0	1	0.971	11.22	138	1	1.06	0.94
3	1	39	10	0	0	1	0.968	11.56	138	1	1.06	0.94
4	2	39	12	0	0	1	0.998	15.28	138	1	1.06	0.94
5	1	0	0	0	-40	1	1.002	15.73	138	1	1.06	0.94
6	2	52	22	0	0	1	0.99	13	138	1	1.06	0.94
7	1	19	2	0	0	1	0.989	12.56	138	1	1.06	0.94
8	2	28	0	0	0	1	1.015	20.77	345	1	1.06	0.94
9	1	0	0	0	0	1	1.043	28.02	345	1	1.06	0.94
10	2	0	0	0	0	1	1.05	35.61	345	1	1.06	0.94
11	1	70	23	0	0	1	0.985	12.72	138	1	1.06	0.94
12	2	47	10	0	0	1	0.99	12.2	138	1	1.06	0.94
13	1	34	16	0	0	1	0.968	11.35	138	1	1.06	0.94
14	1	14	1	0	0	1	0.984	11.5	138	1	1.06	0.94
15	2	90	30	0	0	1	0.97	11.23	138	1	1.06	0.94
16	1	25	10	0	0	1	0.984	11.91	138	1	1.06	0.94
17	1	11	3	0	0	1	0.995	13.74	138	1	1.06	0.94
18	2	60	34	0	0	1	0.973	11.53	138	1	1.06	0.94
19	2	45	25	0	0	1	0.963	11.05	138	1	1.06	0.94
20	1	18	3	0	0	1	0.958	11.93	138	1	1.06	0.94
21	1	14	8	0	0	1	0.959	13.52	138	1	1.06	0.94
22	1	10	5	0	0	1	0.97	16.08	138	1	1.06	0.94
23	1	7	3	0	0	1	1	21	138	1	1.06	0.94
24	2	13	0	0	0	1	0.992	20.89	138	1	1.06	0.94
25	2	0	0	0	0	1	1.05	27.93	138	1	1.06	0.94
26	2	0	0	0	0	1	1.015	29.71	345	1	1.06	0.94
27	2	71	13	0	0	1	0.968	15.35	138	1	1.06	0.94
28	1	17	7	0	0	1	0.962	13.62	138	1	1.06	0.94
29	1	24	4	0	0	1	0.963	12.63	138	1	1.06	0.94
30	1	0	0	0	0	1	0.968	18.79	345	1	1.06	0.94
31	2	43	27	0	0	1	0.967	12.75	138	1	1.06	0.94
32	2	59	23	0	0	1	0.964	14.8	138	1	1.06	0.94

33	1	23	9	0	0	1	0.972	10.63	138	1	1.06	0.94
34	2	59	26	0	14	1	0.986	11.3	138	1	1.06	0.94
35	1	33	9	0	0	1	0.981	10.87	138	1	1.06	0.94
36	2	31	17	0	0	1	0.98	10.87	138	1	1.06	0.94
37	1	0	0	0	-25	1	0.992	11.77	138	1	1.06	0.94
38	1	0	0	0	0	1	0.962	16.91	345	1	1.06	0.94
39	1	27	11	0	0	1	0.97	8.41	138	1	1.06	0.94
40	2	66	23	0	0	1	0.97	7.35	138	1	1.06	0.94
41	1	37	10	0	0	1	0.967	6.92	138	1	1.06	0.94
42	2	96	23	0	0	1	0.985	8.53	138	1	1.06	0.94
43	1	18	7	0	0	1	0.978	11.28	138	1	1.06	0.94
44	1	16	8	0	10	1	0.985	13.82	138	1	1.06	0.94
45	1	53	22	0	10	1	0.987	15.67	138	1	1.06	0.94
46	2	28	10	0	10	1	1.005	18.49	138	1	1.06	0.94
47	1	34	0	0	0	1	1.017	20.73	138	1	1.06	0.94
48	1	20	11	0	15	1	1.021	19.93	138	1	1.06	0.94
49	2	87	30	0	0	1	1.025	20.94	138	1	1.06	0.94
50	1	17	4	0	0	1	1.001	18.9	138	1	1.06	0.94
51	1	17	8	0	0	1	0.967	16.28	138	1	1.06	0.94
52	1	18	5	0	0	1	0.957	15.32	138	1	1.06	0.94
53	1	23	11	0	0	1	0.946	14.35	138	1	1.06	0.94
54	2	113	32	0	0	1	0.955	15.26	138	1	1.06	0.94
55	2	63	22	0	0	1	0.952	14.97	138	1	1.06	0.94
56	2	84	18	0	0	1	0.954	15.16	138	1	1.06	0.94
57	1	12	3	0	0	1	0.971	16.36	138	1	1.06	0.94
58	1	12	3	0	0	1	0.959	15.51	138	1	1.06	0.94
59	2	277	113	0	0	1	0.985	19.37	138	1	1.06	0.94
60	1	78	3	0	0	1	0.993	23.15	138	1	1.06	0.94
61	2	0	0	0	0	1	0.995	24.04	138	1	1.06	0.94
62	2	77	14	0	0	1	0.998	23.43	138	1	1.06	0.94
63	1	0	0	0	0	1	0.969	22.75	345	1	1.06	0.94
64	1	0	0	0	0	1	0.984	24.52	345	1	1.06	0.94
65	2	0	0	0	0	1	1.005	27.65	345	1	1.06	0.94
66	2	39	18	0	0	1	1.05	27.48	138	1	1.06	0.94
67	1	28	7	0	0	1	1.02	24.84	138	1	1.06	0.94
68	1	0	0	0	0	1	1.003	27.55	345	1	1.06	0.94
69	3	0	0	0	0	1	1.035	30	138	1	1.06	0.94
70	2	66	20	0	0	1	0.984	22.58	138	1	1.06	0.94
71	1	0	0	0	0	1	0.987	22.15	138	1	1.06	0.94
72	2	12	0	0	0	1	0.98	20.98	138	1	1.06	0.94
73	2	6	0	0	0	1	0.991	21.94	138	1	1.06	0.94
74	2	68	27	0	12	1	0.958	21.64	138	1	1.06	0.94

75	1	47	11	0	0	1	0.967	22.91	138	1	1.06	0.94
76	2	68	36	0	0	1	0.943	21.77	138	1	1.06	0.94
77	2	61	28	0	0	1	1.006	26.72	138	1	1.06	0.94
78	1	71	26	0	0	1	1.003	26.42	138	1	1.06	0.94
79	1	39	32	0	20	1	1.009	26.72	138	1	1.06	0.94
80	2	130	26	0	0	1	1.04	28.96	138	1	1.06	0.94
81	1	0	0	0	0	1	0.997	28.1	345	1	1.06	0.94
82	1	54	27	0	20	1	0.989	27.24	138	1	1.06	0.94
83	1	20	10	0	10	1	0.985	28.42	138	1	1.06	0.94
84	1	11	7	0	0	1	0.98	30.95	138	1	1.06	0.94
85	2	24	15	0	0	1	0.985	32.51	138	1	1.06	0.94
86	1	21	10	0	0	1	0.987	31.14	138	1	1.06	0.94
87	2	0	0	0	0	1	1.015	31.4	161	1	1.06	0.94
88	1	48	10	0	0	1	0.987	35.64	138	1	1.06	0.94
89	2	0	0	0	0	1	1.005	39.69	138	1	1.06	0.94
90	2	163	42	0	0	1	0.985	33.29	138	1	1.06	0.94
91	2	10	0	0	0	1	0.98	33.31	138	1	1.06	0.94
92	2	65	10	0	0	1	0.993	33.8	138	1	1.06	0.94
93	1	12	7	0	0	1	0.987	30.79	138	1	1.06	0.94
94	1	30	16	0	0	1	0.991	28.64	138	1	1.06	0.94
95	1	42	31	0	0	1	0.981	27.67	138	1	1.06	0.94
96	1	38	15	0	0	1	0.993	27.51	138	1	1.06	0.94
97	1	15	9	0	0	1	1.011	27.88	138	1	1.06	0.94
98	1	34	8	0	0	1	1.024	27.4	138	1	1.06	0.94
99	2	42	0	0	0	1	1.01	27.04	138	1	1.06	0.94
100	2	37	18	0	0	1	1.017	28.03	138	1	1.06	0.94
101	1	22	15	0	0	1	0.993	29.61	138	1	1.06	0.94
102	1	5	3	0	0	1	0.991	32.3	138	1	1.06	0.94
103	2	23	16	0	0	1	1.001	24.44	138	1	1.06	0.94
104	2	38	25	0	0	1	0.971	21.69	138	1	1.06	0.94
105	2	31	26	0	20	1	0.965	20.57	138	1	1.06	0.94
106	1	43	16	0	0	1	0.962	20.32	138	1	1.06	0.94
107	2	50	12	0	6	1	0.952	17.53	138	1	1.06	0.94
108	1	2	1	0	0	1	0.967	19.38	138	1	1.06	0.94
109	1	8	3	0	0	1	0.967	18.93	138	1	1.06	0.94
110	2	39	30	0	6	1	0.973	18.09	138	1	1.06	0.94
111	2	0	0	0	0	1	0.98	19.74	138	1	1.06	0.94
112	2	68	13	0	0	1	0.975	14.99	138	1	1.06	0.94
113	2	6	0	0	0	1	0.993	13.74	138	1	1.06	0.94
114	1	8	3	0	0	1	0.96	14.46	138	1	1.06	0.94
115	1	22	7	0	0	1	0.96	14.46	138	1	1.06	0.94
116	2	184	0	0	0	1	1.005	27.12	138	1	1.06	0.94

117	1	20	8	0	0	1	0.974	10.67	138	1	1.06	0.94
118	1	33	15	0	0	1	0.949	21.92	138	1	1.06	0.94

Table A.7: IEEE 118-bus generator data

bus	Pg	Qg	Qmax	Qmin	Vg	mBase	status	Pmax	Pmin
1	0	0	15	-5	0.955	100	1	100	0
4	0	0	300	-300	0.998	100	1	100	0
6	0	0	50	-13	0.99	100	1	100	0
8	0	0	300	-300	1.015	100	1	100	0
10	450	0	200	-147	1.05	100	1	550	0
12	85	0	120	-35	0.99	100	1	185	0
15	0	0	30	-10	0.97	100	1	100	0
18	0	0	50	-16	0.973	100	1	100	0
19	0	0	24	-8	0.962	100	1	100	0
24	0	0	300	-300	0.992	100	1	100	0
25	220	0	140	-47	1.05	100	1	320	0
26	314	0	1000	-1000	1.015	100	1	414	0
27	0	0	300	-300	0.968	100	1	100	0
31	7	0	300	-300	0.967	100	1	107	0
32	0	0	42	-14	0.963	100	1	100	0
34	0	0	24	-8	0.984	100	1	100	0
36	0	0	24	-8	0.98	100	1	100	0
40	0	0	300	-300	0.97	100	1	100	0
42	0	0	300	-300	0.985	100	1	100	0
46	19	0	100	-100	1.005	100	1	119	0
49	204	0	210	-85	1.025	100	1	304	0
54	48	0	300	-300	0.955	100	1	148	0
55	0	0	23	-8	0.952	100	1	100	0
56	0	0	15	-8	0.954	100	1	100	0
59	155	0	180	-60	0.985	100	1	255	0
61	160	0	300	-100	0.995	100	1	260	0
62	0	0	20	-20	0.998	100	1	100	0
65	391	0	200	-67	1.005	100	1	491	0
66	392	0	200	-67	1.05	100	1	492	0
69	516.4	0	300	-300	1.035	100	1	805.2	0
70	0	0	32	-10	0.984	100	1	100	0
72	0	0	100	-100	0.98	100	1	100	0
73	0	0	100	-100	0.991	100	1	100	0

74	0	0	9	-6	0.958	100	1	100	0
76	0	0	23	-8	0.943	100	1	100	0
77	0	0	70	-20	1.006	100	1	100	0
80	477	0	280	-165	1.04	100	1	577	0
85	0	0	23	-8	0.985	100	1	100	0
87	4	0	1000	-100	1.015	100	1	104	0
89	607	0	300	-210	1.005	100	1	707	0
90	0	0	300	-300	0.985	100	1	100	0
91	0	0	100	-100	0.98	100	1	100	0
92	0	0	9	-3	0.99	100	1	100	0
99	0	0	100	-100	1.01	100	1	100	0
100	252	0	155	-50	1.017	100	1	352	0
103	40	0	40	-15	1.01	100	1	140	0
104	0	0	23	-8	0.971	100	1	100	0
105	0	0	23	-8	0.965	100	1	100	0
107	0	0	200	-200	0.952	100	1	100	0
110	0	0	23	-8	0.973	100	1	100	0
111	36	0	1000	-100	0.98	100	1	136	0
112	0	0	1000	-100	0.975	100	1	100	0
113	0	0	200	-100	0.993	100	1	100	0
116	0	0	1000	-1000	1.005	100	1	100	0

Table A.8: IEEE 118-bus branch data

fbus	tbus	r	x	b
1	2	0.0303	0.0999	0.0254
1	3	0.0129	0.0424	0.01082
4	5	0.00176	0.00798	0.0021
3	5	0.0241	0.108	0.0284
5	6	0.0119	0.054	0.01426
6	7	0.00459	0.0208	0.0055
8	9	0.00244	0.0305	1.162
8	5	0	0.0267	0
9	10	0.00258	0.0322	1.23
4	11	0.0209	0.0688	0.01748
5	11	0.0203	0.0682	0.01738
11	12	0.00595	0.0196	0.00502
2	12	0.0187	0.0616	0.01572
3	12	0.0484	0.16	0.0406

7	12	0.00862	0.034	0.00874
11	13	0.02225	0.0731	0.01876
12	14	0.0215	0.0707	0.01816
13	15	0.0744	0.2444	0.06268
14	15	0.0595	0.195	0.0502
12	16	0.0212	0.0834	0.0214
15	17	0.0132	0.0437	0.0444
16	17	0.0454	0.1801	0.0466
17	18	0.0123	0.0505	0.01298
18	19	0.01119	0.0493	0.01142
19	20	0.0252	0.117	0.0298
15	19	0.012	0.0394	0.0101
20	21	0.0183	0.0849	0.0216
21	22	0.0209	0.097	0.0246
22	23	0.0342	0.159	0.0404
23	24	0.0135	0.0492	0.0498
23	25	0.0156	0.08	0.0864
26	25	0	0.0382	0
25	27	0.0318	0.163	0.1764
27	28	0.01913	0.0855	0.0216
28	29	0.0237	0.0943	0.0238
30	17	0	0.0388	0
8	30	0.00431	0.0504	0.514
26	30	0.00799	0.086	0.908
17	31	0.0474	0.1563	0.0399
29	31	0.0108	0.0331	0.0083
23	32	0.0317	0.1153	0.1173
31	32	0.0298	0.0985	0.0251
27	32	0.0229	0.0755	0.01926
15	33	0.038	0.1244	0.03194
19	34	0.0752	0.247	0.0632
35	36	0.00224	0.0102	0.00268
35	37	0.011	0.0497	0.01318
33	37	0.0415	0.142	0.0366
34	36	0.00871	0.0268	0.00568
34	37	0.00256	0.0094	0.00984
38	37	0	0.0375	0
37	39	0.0321	0.106	0.027
37	40	0.0593	0.168	0.042
30	38	0.00464	0.054	0.422
39	40	0.0184	0.0605	0.01552
40	41	0.0145	0.0487	0.01222

40	42	0.0555	0.183	0.0466
41	42	0.041	0.135	0.0344
43	44	0.0608	0.2454	0.06068
34	43	0.0413	0.1681	0.04226
44	45	0.0224	0.0901	0.0224
45	46	0.04	0.1356	0.0332
46	47	0.038	0.127	0.0316
46	48	0.0601	0.189	0.0472
47	49	0.0191	0.0625	0.01604
42	49	0.0715	0.323	0.086
42	49	0.0715	0.323	0.086
45	49	0.0684	0.186	0.0444
48	49	0.0179	0.0505	0.01258
49	50	0.0267	0.0752	0.01874
49	51	0.0486	0.137	0.0342
51	52	0.0203	0.0588	0.01396
52	53	0.0405	0.1635	0.04058
53	54	0.0263	0.122	0.031
49	54	0.073	0.289	0.0738
49	54	0.0869	0.291	0.073
54	55	0.0169	0.0707	0.0202
54	56	0.00275	0.00955	0.00732
55	56	0.00488	0.0151	0.00374
56	57	0.0343	0.0966	0.0242
50	57	0.0474	0.134	0.0332
56	58	0.0343	0.0966	0.0242
51	58	0.0255	0.0719	0.01788
54	59	0.0503	0.2293	0.0598
56	59	0.0825	0.251	0.0569
56	59	0.0803	0.239	0.0536
55	59	0.04739	0.2158	0.05646
59	60	0.0317	0.145	0.0376
59	61	0.0328	0.15	0.0388
60	61	0.00264	0.0135	0.01456
60	62	0.0123	0.0561	0.01468
61	62	0.00824	0.0376	0.0098
63	59	0	0.0386	0
63	64	0.00172	0.02	0.216
64	61	0	0.0268	0
38	65	0.00901	0.0986	1.046
64	65	0.00269	0.0302	0.38
49	66	0.018	0.0919	0.0248

49	66	0.018	0.0919	0.0248
62	66	0.0482	0.218	0.0578
62	67	0.0258	0.117	0.031
65	66	0	0.037	0
66	67	0.0224	0.1015	0.02682
65	68	0.00138	0.016	0.638
47	69	0.0844	0.2778	0.07092
49	69	0.0985	0.324	0.0828
68	69	0	0.037	0
69	70	0.03	0.127	0.122
24	70	0.00221	0.4115	0.10198
70	71	0.00882	0.0355	0.00878
24	72	0.0488	0.196	0.0488
71	72	0.0446	0.18	0.04444
71	73	0.00866	0.0454	0.01178
70	74	0.0401	0.1323	0.03368
70	75	0.0428	0.141	0.036
69	75	0.0405	0.122	0.124
74	75	0.0123	0.0406	0.01034
76	77	0.0444	0.148	0.0368
69	77	0.0309	0.101	0.1038
75	77	0.0601	0.1999	0.04978
77	78	0.00376	0.0124	0.01264
78	79	0.00546	0.0244	0.00648
77	80	0.017	0.0485	0.0472
77	80	0.0294	0.105	0.0228
79	80	0.0156	0.0704	0.0187
68	81	0.00175	0.0202	0.808
81	80	0	0.037	0
77	82	0.0298	0.0853	0.08174
82	83	0.0112	0.03665	0.03796
83	84	0.0625	0.132	0.0258
83	85	0.043	0.148	0.0348
84	85	0.0302	0.0641	0.01234
85	86	0.035	0.123	0.0276
86	87	0.02828	0.2074	0.0445
85	88	0.02	0.102	0.0276
85	89	0.0239	0.173	0.047
88	89	0.0139	0.0712	0.01934
89	90	0.0518	0.188	0.0528
89	90	0.0238	0.0997	0.106
90	91	0.0254	0.0836	0.0214

89	92	0.0099	0.0505	0.0548
89	92	0.0393	0.1581	0.0414
91	92	0.0387	0.1272	0.03268
92	93	0.0258	0.0848	0.0218
92	94	0.0481	0.158	0.0406
93	94	0.0223	0.0732	0.01876
94	95	0.0132	0.0434	0.0111
80	96	0.0356	0.182	0.0494
82	96	0.0162	0.053	0.0544
94	96	0.0269	0.0869	0.023
80	97	0.0183	0.0934	0.0254
80	98	0.0238	0.108	0.0286
80	99	0.0454	0.206	0.0546
92	100	0.0648	0.295	0.0472
94	100	0.0178	0.058	0.0604
95	96	0.0171	0.0547	0.01474
96	97	0.0173	0.0885	0.024
98	100	0.0397	0.179	0.0476
99	100	0.018	0.0813	0.0216
100	101	0.0277	0.1262	0.0328
92	102	0.0123	0.0559	0.01464
101	102	0.0246	0.112	0.0294
100	103	0.016	0.0525	0.0536
100	104	0.0451	0.204	0.0541
103	104	0.0466	0.1584	0.0407
103	105	0.0535	0.1625	0.0408
100	106	0.0605	0.229	0.062
104	105	0.00994	0.0378	0.00986
105	106	0.014	0.0547	0.01434
105	107	0.053	0.183	0.0472
105	108	0.0261	0.0703	0.01844
106	107	0.053	0.183	0.0472
108	109	0.0105	0.0288	0.0076
103	110	0.03906	0.1813	0.0461
109	110	0.0278	0.0762	0.0202
110	111	0.022	0.0755	0.02
110	112	0.0247	0.064	0.062
17	113	0.00913	0.0301	0.00768
32	113	0.0615	0.203	0.0518
32	114	0.0135	0.0612	0.01628
27	115	0.0164	0.0741	0.01972
114	115	0.0023	0.0104	0.00276

68	116	0.00034	0.00405	0.164
12	117	0.0329	0.14	0.0358
75	118	0.0145	0.0481	0.01198
76	118	0.0164	0.0544	0.01356

Table A.9: IEEE 118-bus generator cost data

bus	c_2	c_1
1	0.01	40
4	0.01	40
6	0.01	40
8	0.01	40
10	0.0222222	20
12	0.117647	20
15	0.01	40
18	0.01	40
19	0.01	40
24	0.01	40
25	0.0454545	20
26	0.0318471	20
27	0.01	40
31	1.42857	20
32	0.01	40
34	0.01	40
36	0.01	40
40	0.01	40
42	0.01	40
46	0.526316	20
49	0.0490196	20
54	0.208333	20
55	0.01	40
56	0.01	40
59	0.0645161	20
61	0.0625	20
62	0.01	40
65	0.0255754	20
66	0.0255102	20
69	0.0193648	20
70	0.01	40

72	0.01	40
73	0.01	40
74	0.01	40
76	0.01	40
77	0.01	40
80	0.0209644	20
85	0.01	40
87	2.5	20
89	0.0164745	20
90	0.01	40
91	0.01	40
92	0.01	40
99	0.01	40
100	0.0396825	20
103	0.25	20
104	0.01	40
105	0.01	40
107	0.01	40
110	0.01	40
111	0.277778	20
112	0.01	40
113	0.01	40
116	0.01	40

Table A.10: IEEE 118-bus storage data for every storage unit

max. storage	min. storage	max. storage rate	min. storage rate	initial storage	final storage
32 MWh	0 MWh	8 MW	-8 MW	0	0

BIBLIOGRAPHY

- [1] T. Yau, L.N. Walker, H. L. Graham, and R. Raithel, "Effects of battery storage devices on power system dispatch," *IEEE Trans. Power Apparatus and Systems*, vol. PAS-100, no. 1, pp. 375-383, Jan. 1981.
- [2] K. Heussen, S. Koch, A. Ulbig, and G. Andersson, "Energy storage in power system operation: The power nodes modeling framework," *IEEE Conf. Publications*, pp. 1-8, 2010.
- [3] E. Sortomme and M. A. El-Sharkawi, "Optimal power flow for a system of microgrids with controllable loads and battery storage," *IEEE Conf. Publications*, pp. 1-5, 2009.
- [4] J. P. Barton and D. G. Infield, "Energy storage and its use with intermittent renewable energy," *IEEE Trans. Energy Conversion*, vol. 19, no. 2, pp. 441-448, June 2004.
- [5] Y. M. Atwa and E. F. El-Saadany, "Optimal allocation of ESS in distribution systems with a high penetration of wind energy," *IEEE Trans. Power Syst.*, vol. 25, no. 4, pp. 1815-1822, Nov. 2010.
- [6] D. Gayme and U. Topcu, "Optimal power flow with large-scale storage integration," *IEEE Trans. Power Syst.*, vol. 28, no. 2, pp. 709-717, 2013.
- [7] J. Lavaei and S. H. Low, "Convexification of optimal power flow problem," *Forty-Eighth Annual Allerton Conf.*, pp. 223-232, Oct. 2010.
- [8] J. Löfberg, "YALMIP: A toolbox for modeling and optimization in MATLAB," *IEEE International Symposium on Computer Aided Control Systems Design*, pp. 284-289, Sept. 2004.
- [9] J. F. Sturm, "Using SeDuMi 1.02, A MATLAB toolbox for optimization over symmetric cones," *Overseas Publishers Association, Optimization Meth. & Soft.*, vol. 11&12, pp. 625-653, Mar. 1999.
- [10] D. Gayme and U. Topcu, "Optimal power flow with distributed energy storage dynamics," *American Control Conf.*, pp. 1536-1542, Jul. 2011.
- [11] K. M. Chandy, S. H. Low, U. Topcu, and H. Xu, "A simple optimal power flow model with energy storage," *49th IEEE Conf. Decision and Control*, pp. 1051-1057, Dec. 2010.
- [12] E. Sjodin, D. F. Gayme, and U. Topcu, "Risk-mitigated optimal power flow for wind powered grids," *American Control Conf.*, pp. 4431-4437, June 2012.

- [13] H. Oh, "Optimal planning to include storage devices in power systems," *IEEE Trans. Power Systems*, vol. 26, no. 3, pp. 1118-1128, Aug. 2011.
- [14] The MOSEK optimization toolbox for MATLAB manual, Version 6.0 (Revision 148), MOSEK ApS, Denmark. [Online]. Available: <http://www.mosek.com>.
- [15] University of Washington, Power System Test Case Archive. [Online]. Available: <http://www.ee.washington.edu/research/pstca>.
- [16] D. Bertsimas, D. Pachamanova, and M. Sim, "Robust linear optimization under general norms," *Operations Research Letters*, vol. 32, no. 6, pp. 510-516, Nov. 2004. [Online]. Available: <http://www.sciencedirect.com/science/article/pii/S0167637704000082>.
- [17] V. Guigues, "Robust production management," Optimization Online, Feb. 2011.
- [18] R. A. Jabr, "Adjustable robust OPF with renewable energy sources," *IEEE Trans. Power Syst.*, vol. 28, no. 4, pp. 4742-4751, Nov. 2013.
- [19] M. Madrigal, K. Ponnambalam, and V. H. Quintana, "Probabilistic optimal power flow," in *Proc. IEEE Canadian Conf. Electrical and Computer Engineering*, May 24-28, 1998, vol. 1, pp. 385-388.
- [20] M. E. El-Hawary and G. A. N. Mbamalu, "Stochastic optimal load flow using a combined quasi-Newton and conjugate gradient technique," *Int. J. Elect. Power Energy Syst.*, vol. 11, no. 2, pp. 85-93, Apr. 1989.
- [21] Z. Hu, X. Wang, and G. Taylor, "Stochastic optimal reactive power dispatch: Formulation and solution method," *Int. J. Elect. Power Energy Syst.*, vol. 32, no. 6, pp. 615-621, Jul. 2010.
- [22] H. Zhang and P. Li, "Probabilistic analysis for optimal power flow under uncertainty," *IET Gener. Transm. Distrib.*, vol. 4, no. 5, pp. 553-561, May 2010.
- [23] Y. Yuan, Q. Li, and W. Wang, "Optimal operation strategy of energy storage unit in wind power integration based on stochastic programming," *IET Renew. Power Gener.*, vol. 5, no. 2, pp. 194-201, Mar. 2011.
- [24] X. Liu, "Economic load dispatch constrained by wind power availability: A wait-and-see approach," *IEEE Trans. Smart Grid*, vol. 1, no. 3, pp. 347-355, Dec. 2010.
- [25] Q. Wang, Y. Guan, and J. Wang, "A chance-constrained two-stage stochastic program for unit commitment with uncertain wind power output," *IEEE Trans. Power Syst.*, vol. 27, no. 1, pp. 206-215, Feb. 2012.
- [26] J. Usaola, "Probabilistic load flow with wind production uncertainty using cumulants and Cornish-Fisher expansion," *Int. J. Elect. Power Energy Syst.*, vol. 31, no. 9, pp. 474-481, Oct. 2009.

- [27] J. Branke, "Creating robust solutions by means of evolutionary algorithms," in *Parallel Problem Solving from Nature*, Springer Berlin Heidelberg, 1998, pp. 119-128.
- [28] H. Madsen, P. Pinson, G. Kariniotakis, H. Nielsen, and T. Nielsen, "Standardizing the performance evaluation of short-term wind power prediction models," *Wind Engineering*, vol. 29, no. 6, pp. 475-489, 2005.
- [29] IBM ILOG CPLEX V 12.5. [Online]. Available: <http://www-01.ibm.com/software/integration/optimization/cplex-optimizer>.
- [30] R. D. Zimmerman, C. E. Murillo-Sanchez, and R. J. Thomas, "MATPOWER: Steady-state operations, planning, and analysis tools for power systems research and education," *IEEE Trans. Power Syst.*, vol. 26, no. 1, pp. 12-19, Feb. 2011.
- [31] H. Yu and W. D. Rosehart, "An optimal power flow algorithm to achieve robust operation considering load and renewable generation uncertainties," *IEEE Trans. Power Syst.*, vol. 27, no. 4, pp. 1808-1817, Nov. 2012.